BRNO UNIVERSITY OF TECHNOLOGY

VYSOKÉ UČENÍ TECHNICKÉ V BRNĚ

CENTRAL EUROPEAN INSTITUTE OF TECHNOLOGY BUT

STŘEDOEVROPSKÝ TECHNOLOGICKÝ INSTITUT VUT

ION-SELECTIVE MEMBRANE WITH ANTIMICROBIAL EFFECT

IONTOVĚ SELEKTIVNÍ MEMBRÁNA S ANTIMIKROBIÁLNÍM ÚČINKEM

DOCTORAL THESIS

DIZERTAČNÍ PRÁCE

AUTHOR — Ing. Evelína Gablech

AUTOR PRÁCE

SUPERVISOR — doc. Ing. Jana Drbohlavová, Ph.D.

ŠKOLITEL

CO-SUPERVISOR — Ing. Jan Křivčík

ŠKOLITEL SPECIALISTA

BRNO 2022

Abstract

This work deals with improvement of antimicrobial properties of commercial polymer membranes used in dairy industry for filtration of milk products such as whey. These membranes suffer from contamination caused by microorganisms present in milk during the filtration process. This biological contamination affects the life-time of the membrane and also filtration process itself. Thus, these membranes were modified with plasma treatment to incorporate amine functional groups for subsequent immobilization of silver and selenium nanoparticles to prevent the membranes from creation of biofilm of microorganisms. Antimicrobial activity of both types of nanoparticles and membranes with immobilized nanoparticles was determined against cell strains *Staphylococcus aureus* and *Escherichia coli*.

Abstrakt

Tato práce se zabývá zlepšením antimikrobiálních vlastností komerčních polymerních membrán používaných v mlékárenském průmyslu pro filtraci mléčných výrobků jako je syrovátka. Tyto membrány trpí kontaminací způsobenou mikroorganismy přítomnými v mléce během procesu filtrace. Toto biologické znečištění ovlivňuje životnost membrány i samotný filtrační proces. Pro ochranu membrány před vytvořením biofilmu z mikroorganismů byly tyto membrány modifikovány pomocí plazmových metod tak, aby došlo k funkcionalizaci aminovými skupinami pro následnou imobilizaci nanočástic stříbra a selenu. Antimikrobiální aktivita obou typů nanočástic a membrán s imobilizovanými nanočásticemi byla stanovena proti buněčným kmenům *Staphylococcus aureus* a *Escherichia coli*.

Keywords

Polymer membranes, silver nanoparticles, selenium nanoparticles, plasma treatment, functionalization, antimicrobial activity, cytotoxicity, immobilization of nanoparticles.

Klíčová slova

Polymerní membrány, stříbrné nanočástice, selenové nanočástice, plasmová modifikace, funkcionalizace, antimikrobiální aktivita, cytotoxicita, imobilizace nanočástic.

GABLECH, Evelína. *Iontově selektivní membrána s antimikrobiálním účinkem*. Brno, 2022. Dostupné také z: https://www.vutbr.cz/studenti/zav-prace/detail/143310. Dizertační práce. Vysoké učení technické v Brně, Středoevropský technologický institut VUT, Středoevropský technologický institut VUT. Vedoucí práce Jana Drbohlavová.

DECLARATION

I certify, that I performed dissertation work independently, under the supervision of doc. Ing. Jana Drbohlavová, Ph.D. All technical literature and other information sources presented in this work are properly cited in the text and listed in the reference list.

Brno: 28.2.2022

author´s signature

ACKNOWLEDGEMENT

I would like to thank to my supervisor doc. Ing. Jana Drbohlavová, Ph.D. and my supervisor specialist Ing. Jan Křivčík for their effective technical and pedagogical support and all their valuable advices during my studies a completation of this dissertation thesis.

Last, but not least, I would like to thank to my family for their patience and support during my studies. My thanks belong especially to my husband Imrich.

Brno: 28.2.2022

author´s signature

CONTENT

List of abbreviations

Anex	anion-exchange
Ag NPs	silver nanoparticles
ATP	adenosine triphosphate
AFM	atomic force microscopy
BrdU	bromodeoxyuridine
Catex	cation-exchange
CCM	Czech Collection of Microorganisms
CCP	capacitively coupled plasma
CFU	colony forming units
CPA	cyclopropylamine
DNA	deoxyribonucleic acid
DLS	dynamic light scattering
ED	electrodialysis
FBS	fetal bovine serum
FTIR	Fourier transform infrared spectroscopy
HR-TEM	high resolution transmission electron microscopy
IEM	ion exchange membrane
IR	infra-red
LDH	lactate dehydrogenase
LDPE	low-density
MBC	minimum bactericidal concentration
MH Broth	Mueller-Hinton broth
MH Agar	Mueller-Hinton agar
MF	microfiltration
MIC	minimum inhibitory concentration
MPs	membrane processes
MTT	(3-(4,5-dimethylthiazol-2-yl) -2–5-diphenyltetrazolium bromide)
NF	nanofiltration
PEG	polyethylene glycol
PES	polystyrene
PVA	polyvinyl alcohol

PVP	polyvinylpyrrolidone
RF	radio frequency
RIE	reactive ion etching
RO	reverse osmosis
ROS	reactive oxygen species
SAXS	small angle X-ray scattering
USAXS	ultra-small angle X-ray scattering
Se NPs	selenium nanoparticles
SD	standard deviation
SDS	sodium dodecyl sulfate
SEM	scanning electron microscopy
SPR	surface plasmon resonance
TEM	transmission electron microscopy
UF	ultrafiltration
XRD	X-ray diffraction
XTT	(2,3-bis-(2-methoxy-4-nitro-5-sulfophenyl)-2H-tetrazolium-5-carboxanilide)

1 Introduction

The current issue in a dairy industry is how to keep a filtration process of milk products free from bacterial contamination. The most common treatments of milk products utilizes membrane processes (MPs) [1, 2]. Big advantage of MPs is a loss of very small amount of bioactive substances (such as microorganisms etc.) because the filtration is held under lower temperatures, chemical composition is preserved, energy consumption is low, as well as sensoric properties remain the same [3, 4]. MPs in dairy industry are exploited for removing of fat and microorganisms, decreasing of undesirable agents (lactose), enriching of milk with several components (whey proteins) or increasing the yield of milk products (desalination of whey) [1, 5]. One of the most important problem of the MPs is degradation of membrane during working conditions, namely congesting and biofouling caused by microorganisms creating biofilm on the surface of the membrane. This pollution very negatively affects an effectivity of filtration process and life time of the membrane [6, 7]. One of the frequent applications of these filtration membranes is desalination process of whey. The whey, contains very high amount of bioactive and organic components, which in combination with demands on membrane properties bring a lot of technological challenges [8, 9]. In practice, to avoid contamination of membranes, they are purified mechanically or with various aggressive chemicals such as oxidizing agents or acids, which can damage membrane as well. However, science brings new possibilities that can significantly prolong not only the life time of the membrane, but also can preserve the effectivity of MPs [7, 10].

Novel attitudes lately reported in few scientific papers how to prevent the membranes from biofouling including surface modification with various types of nanoparticles [11]. Nowadays, nanochemistry frequently uses nanoparticles with unique properties compared to their macro-scaled counterparts coming from their high surface to volume ratio [12, 13]. In general, nanoparticles are clusters of atoms with size in the range of 1-100 nm [14-16]. Specifically for antimicrobial application, it seems that silver nanoparticles (Ag NPs) and selenium nanoparticles (Se NPs) are the best candidates [17, 18].

The antibacterial effect of Ag NPs and Se NPs is very closely interconnected with their size; general postulate is that the smaller is the NPs, the higher is the antibacterial activity [19]. It is also well-known that silver-based materials are significantly toxic to microorganisms; such as *Staphylococcus aureus* or *Escherichia coli* [20, 21]. The newest research related to the safety of nanomaterials however shows that Ag NPs are being more and more questioned due to their significant environmental impact, especially to organisms living in the soil and aquatic ecosystems [22]. That is why the scientists are looking for an alternative candidate with less harmful impact to environment and human health.

Selenium (Se) is an essential micronutrient and in low concentrations very important and non-toxic to human body. Se NPs evince also promising biological properties such as very strong antimicrobial effect. Se NPs are able to defuse organisms such as *S. aureus* or *E. coli* [23, 24]..

2 Aims of thesis

This thesis was realized in a cooperation with company MemBrain, ltd [25]. The company produces the commercial polymer ion-exchange membranes used in food industry for desalination of whey and for filtration of milk products. These membranes suffer during desalination process from the contamination with bacteria that create a biofilm, which damage and congest the membrane pores and subsequently debase not only membrane quality and life- time but also filtration process.

Milk products consist of a very high number of biological organisms, which can affect the MPs and also the condition of the membrane. Aim of this thesis is to modify the membrane to achieve antimicrobial properties. Thus, NPs were immobilized on the polymer membrane to prevent it from the contamination and eventually from degradation, as well.

Crucial part of this thesis was to find the proper antimicrobial agent. Ag NPs and Se NPs were chosen because of their very well-known antimicrobial properties.

To achieve the main goal, the thesis pursued the following specific objectives and activities:

1. The synthesis of Ag and Se NPs and their optimization to achieve the desired properties for subsequent utilization in membrane modification - most importantly the colloidal stability and suitable toxicological properties. The optimization process was based on tuning the physico-chemical properties of NPs via following synthesis parameters: concentration of reagents, utilization of different stabilizing substances, reaction conditions such as temperature or interaction with UV light. The prepared NPs were characterized by various methods determine their morphology: size and size distribution, shape as well as colloidal stability.
2. In the next step cytotoxicity of both types of Ag NPs and Se NPs were performed.
3. Subsequently, the antimicrobial tests were performed to prove the NPs antimicrobial effect.
4. The next part of this thesis was dedicated to the challenging immobilization of NPs onto polymer membrane. This stage included the plasma modification of surface of the polymer membranes to incorporate the desired functional groups for subsequent immobilization of NPs.
5. In the last part, polymer membranes with immobilized NPs were tested to determine the antimicrobial activity.

Company MemBrain ltd. provided two types of polymer membranes: anion-exchange (anex) and cation-exchange (catex). In this thesis only catex membranes were used due to better stability to various chemicals.

3 State of the art

3.1 Membrane processes

Membrane technologies are widely used in industries such as food, paper, and textile industry, pharmacy, biotechnology or chemical industry. In general, food industry employs membrane processes (MPs) because they are easy to process material but also thanks due to their ability to achieve highly selective separations. Dairy industry is one of the areas where MPs are used on the widest scale. They can be utilized in entire spectrum of workflow from primary production and treatment of milk to production of cheese or other milk products. Dairy industry usually uses MPs of first generation, namely based on pressure and usage of electromembrane [1, 2, 26]. These filtration processes can be combined with each other, as well [27]. Membranes are able to catch a huge part of microorganisms but also chemicals such as herbicides, pesticides, dyes, pharmaceuticals or sediments which could negatively affect the final product. Dairy industry utilizes for filtration of milk and whey mostly pressure MPs, namely microfiltration (MF), ultrafiltration (UF), nanofiltration (NF), reverse osmosis (RO) and from electric MP electrodialysis (ED). Principle of pressure MPs lies in utilization of different pressure, properties of membrane and dominant transport mechanism.

Figure 1 shows schematic illustration of separation process of pressure methods.

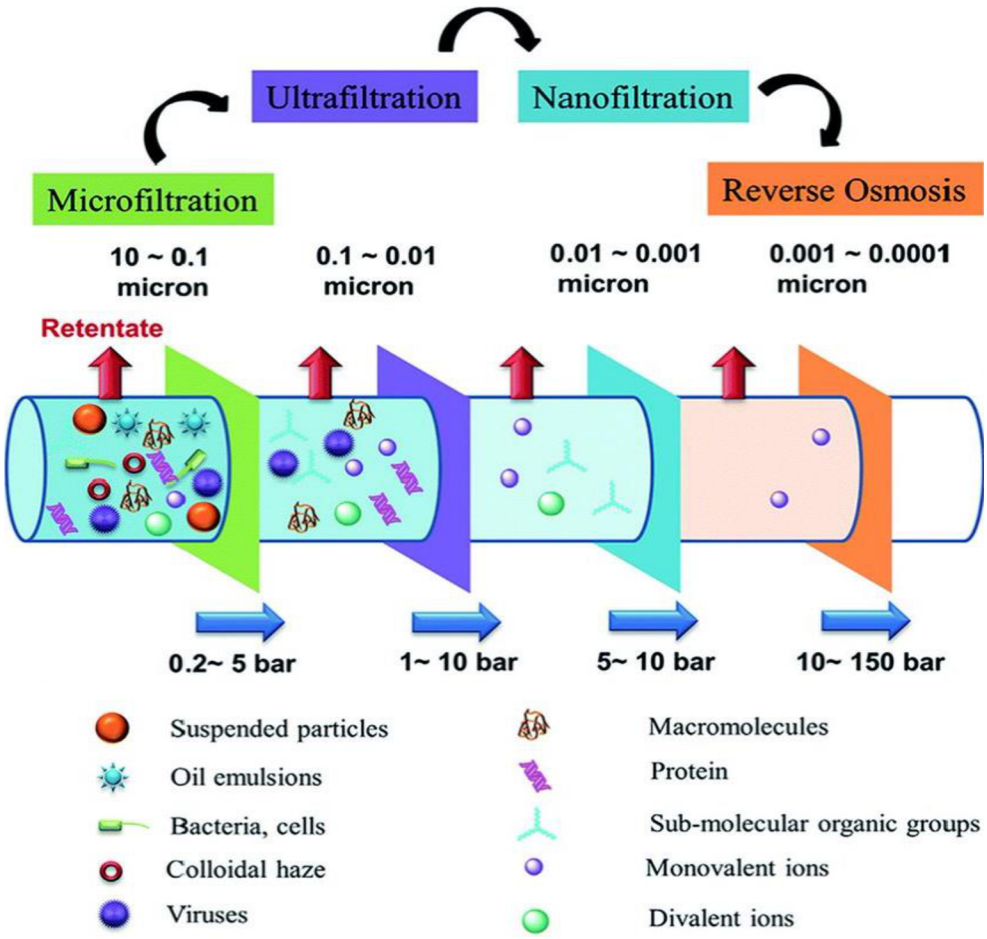

Figure 1: Schematic illustration of pressure membrane processes [27].

Pressure difference, which is used as stimulus above and under membrane causes that low molecular substances get through the membrane and high molecular substances are caught on the membrane. Dimensions of separated particles and molecules decrease in sequence from MF, through UF and NF to RO, hence dimensions of membrane pores decreases as well. It leads to higher pressure of MPs to overcome the membrane resistance against the transport, which keeps constant flow of separation process. Product of separation process is permeate with almost zero concentration of separated component and retentate, where separated components are concentrated. Even though there are significant differences between individual processes, in practice there is no exact boundary between them [27, 28].Electrodialysis depicted in

Figure 2 is a separation process where direct current electric field affects dissociated substances in solvent. Such electrical potential between two electrodes causes movement of positively charged particles to negative electrode and simultaneously negatively charged particles move to positive electrode. Electrodialysis apparatus consist of a diluate chamber, which serves as a channel for depleted stream and concentrate chamber serves as a channel for enriched stream. A real device in working conditions can include a few hundreds of these chambers. Electrodialysis is in dairy industry usually used for processing of whey (for example desalination of whey). MPs can be used in many areas of dairy industry from basic treatment of milk, through thicken the milk or whey to separation of their individual substances (fat, proteins, lactose, mineral salts, etc.) and demineralization [28].

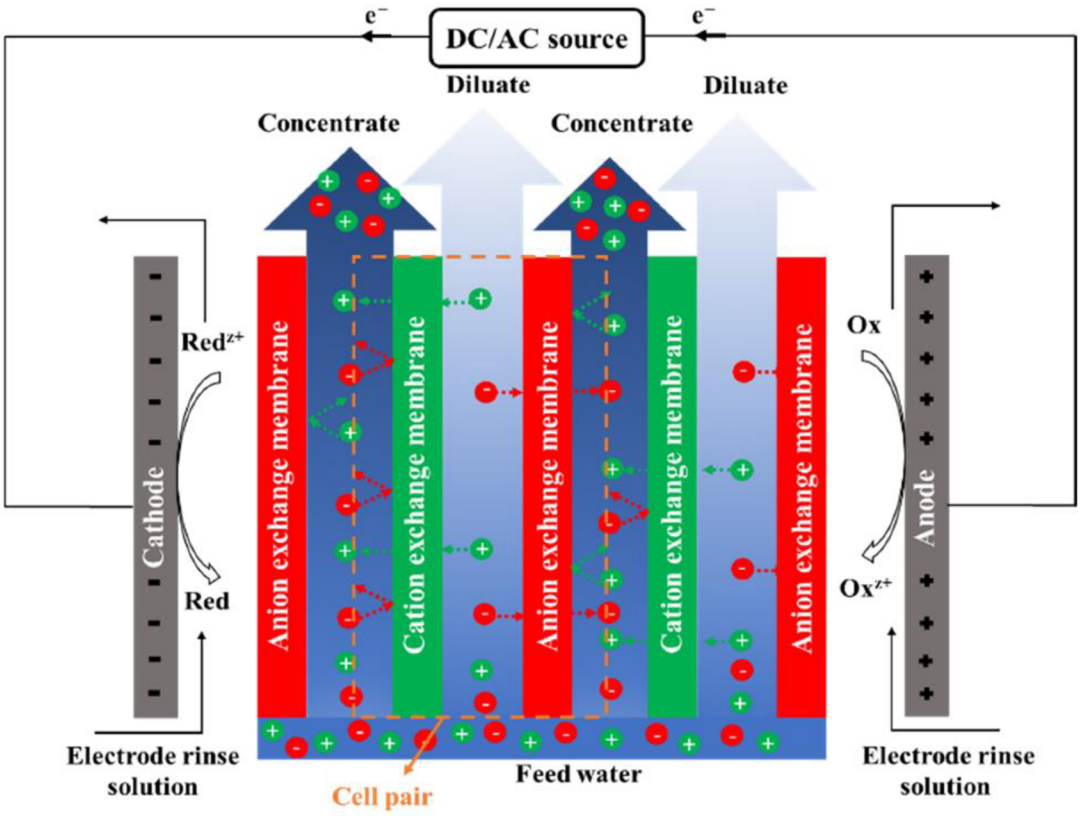

Figure 2: Schematic illustration of electrodialysis [28].

3.2 Membranes used in membrane processes

Membranes used in MPs can be biological or synthetic. Membranes can be divided into several groups based on their properties such as origin, physical state, material (fabrication), structure and morphology [29, 30].

A special type of these membranes is ion exchange membranes (IEM). IEM are usually employed in ED processes. It is a type of membrane, which can transport ions with the same type of charge e.g. positive or negative (this membrane cannot transport neutral molecules or solvent itself) depending on ion-exchange material (ionex) that membrane contains. Charge of functional group in the membrane is compensated with equivalent quantity of opposite charged ions. Filtration of several compounds can be accompanied with penetration of so called counterions, which have the same charge as functional groups in membrane. In milk industry they are used mainly for desalination of whey [31]. IEM can be homogeneous or heterogeneous, and also composites, if there are additional compounds for desired properties. They are also divided into few groups according to type of ionex they contain [31]: **catex** membranes (allow penetration of only positively charged particle, **anex** membranes (allow penetration of only negatively charged particles), **bipolar membranes** - special type, which combines anex and catex layers.

Proper functionality of membrane is driven from its properties such as swelling capacity, thickness, ion exchange capacity, perm selectivity, transfer number, ion conductivity diffuse coefficient, hydraulic resistance, thermal stability, chemical stability and mechanical strength. These are the points that should be considered during development of membranes. The most important properties are high perm selectivity, high permeability and long life-time. Selectivity is very important because it defines the effectivity of selection process and also purity of final product. Permeability defines speed of filtration process. Usually, in working conditions, poor permeability requires membrane with bigger area. Membrane should be resistant to mechanical, chemical and temperature factors and it usually depends on fabrication process and used materials. Selection and suitable utilization of membrane is very related to exact filtration process and it is dependent on many factors.

Generally, versatile membrane for all application does not exist, thus it is very important to consider following demands when it comes to final application: type of MPs, composition of filtered mixtures (dimensions of particles and molecules, properties of solvent), material and properties of membrane, membrane pollution and contamination (scaling, fouling, biofouling), sanitation of membrane, damage of membrane from inappropriate operating conditions and storage of membrane.

A very common problem of IEM (and membranes used in food industry in general) is their contamination and congesting during filtration process, especially in dairy industry, where milk and milk products evince high biological activity. Microorganisms create a biofilm on the surface of the membrane and this is called biofouling [31, 32]. An example of biofouling on polymer membrane is depicted in Figure 3.

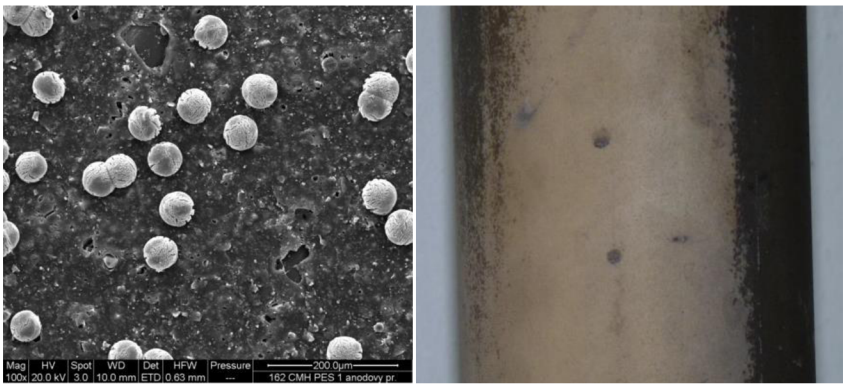

Figure 3: SEM image of polymer membrane with microbial contamination (left), photography of contaminated polymer membrane (right)[31].

3.2.1 Biofouling of polymer membranes - creation of biofilm

As mentioned above, biofouling is a process when bacteria form a thin layer on the surface of polymer membranes (so-called biofilm). This biofilm then negatively impacts not only the properties of the membranes, but also the filtration process itself [33]. Biofilm formation is not yet fully described, especially with respect to the initial phase, but there are several theories how the biofilm from bacteria is formed. Biofilm formation consist of several stages (see Figure 4) [34-36] :

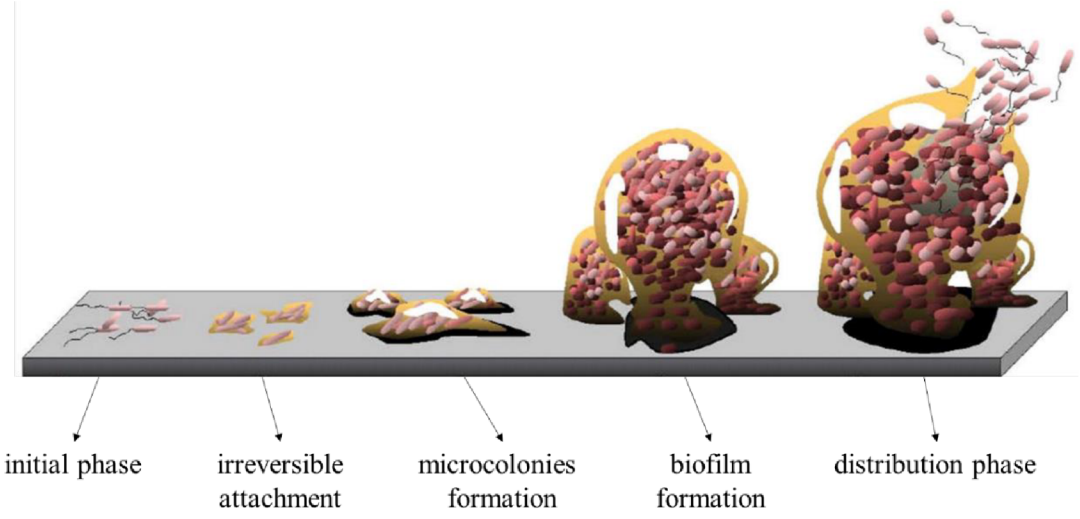

Figure 4: Biofouling process - formation of bacterial biofilm [35].

1. **Initial phase** - this stage can also be called as conditioning stage. At this phase, the bacteria reversibly interact with the polymer surface. When bacteria separate from the surface, there are remaining extracellular compounds on the surface of the membrane. These compound most likely play a significant role in a subsequent formation of biofilm.
2. **Phase of irreversible attachment** - also called as the phase of primary adhesion. In this phase bacteria irreversibly adhere to the surface of the membrane and the bonding is stable.

3. **Microcolonies formation** - also named as the maturing phase 1. In this phase, bacteria multiply and form colonies.
4. **Formation of biofilm** - can be also called as maturing phase 2. This is the phase when cells are completely adhered to the membrane surface and begin to form extracellular substances (mostly based on polysaccharides). When the entire surface is covered with this extracellular substance - a biofilm is formed. At this stage, the biofilm is stable and bacteria can multiply. In their scientific work published by Sedlařík et al. they stated that in order to deactivate the biofilm, it requires 100 times higher concentration of antibiotics in comparison to bacteria that are not part of the biofilm [35].
5. **Distribution phase** - the amount of multiplied bacteria rapidly increased, which cause the rupture of the biofilm. The bacteria are then released into the environment (in this case into milk or the filtered product, respectively)

3.2.2 Polymer membranes for filtration of milk

The basic structure of membranes contains a binder - low density polyethylene (LDPE) and a filler - strong acidic or alkalic ionex based on styrene-divinylbenzene copolymer. The finely milled ionex provides ion conductivity of membrane. Another substance is reinforcing fabric from polystyrene (PES), which significantly affects operating limitations of membranes. The exact ratio and amount of substances of membranes is subject to corporate secret [31].Figure 5 shows swelled catex membrane.

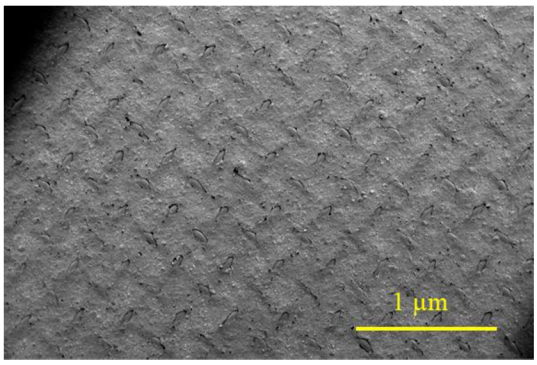

Figure 5: Catex polymer membrane in swelled state [31].

Surface of membrane is mostly smooth. Swelling causes changes in dimension of membranes and finely milled iones, thus surface becomes more structured. Swelling also causes partial crackles on the surface of the membrane, mostly in place of reinforcing fabric [31].

Membranes are fabricated by thermoplastic processing with maximum temperature of 160 °C and maximum pressure of 300–400 bar. Higher temperature than this maximum is not required due to limited temperature tolerance of ionex material [31]. Average working temperature for utilizing of polymer membranes is about 45 °C and pH 0–10 because of the reinforcing textile. Membranes can work only in swelled state (swelling is usually provided in deionized or in drinking water). In general, the higher is the operating temperature, the higher is the transport of salts, which is more advantageous in practical usage in most of application of membranes. For example, membranes can be used for electrodialysis process with high temperature when hot solution is processed, thus it is not necessary to cool it before procedure. Lifetime of membranes depends mostly on the type of application. The lowest lifetime of polymer membranes is usually at food industry and it is about 3 years but it can be 5–7 years for other

applications. The most important parameter for any utilization is immunity to chemical cleaning in acids and alkalics. PES reinforcing textile is sensitive to strong acids or alkalics, so the company tries to decrease concentration and usage of these materials, which is more ecologic, as well. Membranes are preferably used for water solutions without any content of solvents or organic compounds, which could decay membranes. It is recommended to store the membranes at temperature of 5–25 °C in dry, dark place [31].

3.3 Nanoparticles as an antimicrobial agent

3.3.1 Silver nanoparticles as an antimicrobial agent

Silver was used already by ancient Greeks for treatment of ulcers, wound healing and as preservative agent for food and water. In fact, silver was very important antimicrobial material before the antibiotics were found and it is used in various areas till today [37].

Ag NPs have been widely studied during the last decade and they play an important role in nanotechnology. One of the very interesting biological characteristics of silver and Ag NPs is its antibacterial activity. It is well known that silver is very effective against various types of bacteria and microorganisms such as *E. coli* or *S. aureus*, which can cause various diseases such as inflammatory diseases, diarrhea, etc.

The biological activity of Ag NPs depends on their size, size distribution, shape, surface coatings, particle morphology, ion release or agglomeration. Al these factors determine their interactions and impact on final application because they significantly influence their antimicrobial activity and cytotoxicity [38]. Thus, optimization of Ag NPs synthesis is an important step to achieve desired properties such as good colloidal stability (at least 3 weeks due to experiments) and strong antimicrobial properties in order to protect polymer membrane from degradation caused by microorganisms present in milk products and whey. Size is very important because the smaller is the particle, the larger is the surface area to mass ratio, which provides greater interaction with cells or even allows the nanoparticle enter the cell [39]. Several studies revealed that shape of nanoparticles is important, as well. Asymmetric shapes show stronger antimicrobial activity probably due to the specific area that interacts with cell [40]. The overview of various silver nanoparticles used as antimicrobial agent is summarized in the Table 1 below:

Table 1: Silver nanoparticles as antimicrobial agent (PEG - polyethylene glycol, SDS - sodium dodecyl sulphate, MIC - minimum inhibitory concentration, MBC - minimum bacterial concentration, NA - not available).

Ag NPs size and measuring method	**Ag NPs shape and measuring method**	**Chemicals for synthesis (P=precursor, R=reductant, S=stabilizer)**	**Synthesis conditions**	**Microorganisms and type of antimicrobial test**	**Ref.**
NA UV-VIS spectroscopy	NA	P: silver nitrate R: ascorbic acid S: chitosan (also reductant)	Heating in microwave oven (800 W, 4 min)	*B. subtilis*, *E. coli* MIC, MBC	[13]
NA	Spherical	P: silver nitrate R: dextrose	Heating and stirring at	*E. coli, P. aeruginosa* MIC, MBC	[41]

UV-VIS spectroscopy	TEM	S: gelatin	70 °C for several h		
15 nm TEM	Spherical TEM	P: silver nitrate R: sodium borohydride	Vigorous stirring at room temperature	*E. coli* inhibition zones	[42]
5-40 nm TEM	Spherical TEM	Commercial Ag NPs	NA	*E. coli* concentration /contact testing	[43]
9-30 nm TEM	Spherical TEM	P: silver nitrate R: hydrazine hydrate S: sodium citrate or SDS or none	Stirring at room temperature	*S. aureus* MIC, inhibition zones	[19]
10-25 nm TEM	Spherical TEM	P: silver nitrate S and R: PEG	Stirring at room temperature	*S. aureus, S. typhimorium* inhibition zones	[17]
7-15 nm TEM	Spherical TEM	P: silver nitrate R: ethanol S: linoleic acid	Stirring at 70 °C for 2 h	*S. basillus, S. aureus, P. aureginosa* inhibition zones	[44]

3.3.2 Selenium nanoparticles as an antimicrobial agent

Selenium is important semimetal trace element for antioxidation defense and reduces the redox state via specific metabolic pathways. Thus, in the last decades, Se NPs are deeply studied as promising agent for their biomedical potential. Se NPs exhibit low toxicity, degradability and high bioavailability. The major advance of Se NPs is strong ability as regulation of the reactive oxygen species which may trigger of the apoptosis and autophagy.

Se NPs has also potential in suppressing the bacteria activity while directly killing them or blocking the evolution in a specific environment. This can be used for the treatment of bacteria with strong resistance to antibiotics, which is well-known issue of the last years and is predicted to be worse in the following years. Alongside the treatment of bacteria-based diseases, Se NPs can be used as a protection for liquids, which suffer from a high spread of bacteria, hence, the Se NPs are capable to stop or slow down these processes. For example, the milk-based liquids can contain *S. aureus* and *E. coli* that can proliferate at high speed, when these liquids are contaminated or improperly stored, which can be very harmful in case of ingestion. Se NPs are able to stop the biofouling process with high efficiency. Similarly to Ag NPs, the antimicrobial ability of Se NPs is influenced by many factors, such as the dimensions, shape and method of synthesis [45, 46]. Table 2 summarizes preparation procedures and utilization of Se NPs as antimicrobial agent.

Table 2: Selenium nanoparticles as antimicrobial agent (PVA - polyvinylacohol, BSA - bovine serum albumin, DLS - dynamic light scattering, NA - not available).

Se NPs size and measuring method	**Se NPs shape and measuring method**	**Chemicals for synthesis (P=precursor, R=reductant, S=stabilizer)**	**Synthesis conditions**	**Microorganisms and type of antimicrobial test**	**Ref.**
150 nm DLS	Spherical TEM	P: selenium pellets	Pulsed laser ablation	*S. aureus*, *E. coli* - inhibition of growth	[46]

50-80 nm TEM	Spherical TEM	P: sodium selenite	*In vitro* biological synthesis	*E. coli - relative mRNA expression*	[47]
NA	Rods TEM	P: sodium selenite R: ascorbic acid S: PVA	Stirring at 75 °C for 15 min	*E. coli, S. aureus* - inhibition zones	[48]
10-50 nm TEM, DLS	Spherical TEM	P: selenium dioxide	In vitro biological synthesis	*B. cereus, E. faecalis, S. aureus, E. coli, S. typhimurium, and S. Enteritidis* - MIC	[49]
75-300 nm DLS	Spherical SEM	P: sodium selenite R: glucose, ascorbic acid S: chitosan, BSA	Stirring and heating	Gram- positive and Gram-negative bacteria strains - MIC	[50]
40-200 nm TEM	Spherical TEM	P: selenium dioxide R: sodium thiosulfate S: PVA	Stirring at room temperature	*S. aureus* - growth curves, MIC	[51]

3.3.3 Mechanism of antimicrobial effect of silver and selenium nanoparticles

Mechanism of Ag NPs and Se NPs antimicrobial activity is still not very well known and has not been completely explained yet. However, there are few theories and they all have in common few facts. It is believed that the mechanism of interaction with microbial cell is driven mostly from their design, i.e. size, shape, pH, ionic strength and capping medium. The first important fact is how the nanoparticle interacts with the cell and the second how it behaves inside the cell. Scientific papers mostly mention the five following actions: [52-54], adhesion on the surface of the bacterial cell wall and membrane, penetration into the cell via several options such as phagocytosis, simple diffusion, facilitated diffusion, micropinocytosis, clathrin-mediated endocytosis and caveolae-mediated endocytosis, disruption of intracellular organelles and biomolecules, induction of oxidative stress, and modulation of signal transduction pathways. Mechanism of antimicrobial effect of NPs is illustrated in Figure 6.

Some researchers revealed that the Ag NPs and Se NPs can be attracted to cell via electrostatic forces. Due to electrostatic forces and their affinity to iron-sulfur proteins, Ag NPs and Ag ions, as well as the Se NPs can adhere to the cell wall or cytoplasm, which significantly changes the permeability of the cell wall. Consequently, they change the cell membrane arrangements, thus nanoparticles can penetrate through the cell wall or cause the disruption of cell wall. When the nanoparticles enter the inner space of the wall, it negatively affects the respiratory enzymes leading to creation of reactive oxygen species (ROS) and it also interrupts the release of adenosine triphosphate (ATP). ROS could be crucial to affect deoxyribonucleic acid (DNA). When nanoparticles interact with DNA via phosphorus and iron-sulfur, it can lead to changes such as DNA replication, propagation, and DNA damage. Additionally, these nanoparticles probably impede also the synthesis of proteins. Ag NPs and Se NPs can cause a rupture of some organelles, subsequently followed by their lysis. These nanoparticles also interact with thiol groups with many vital enzymes and inactivate them. All these mentioned actions can cause the cell death [15, 39, 55-59].

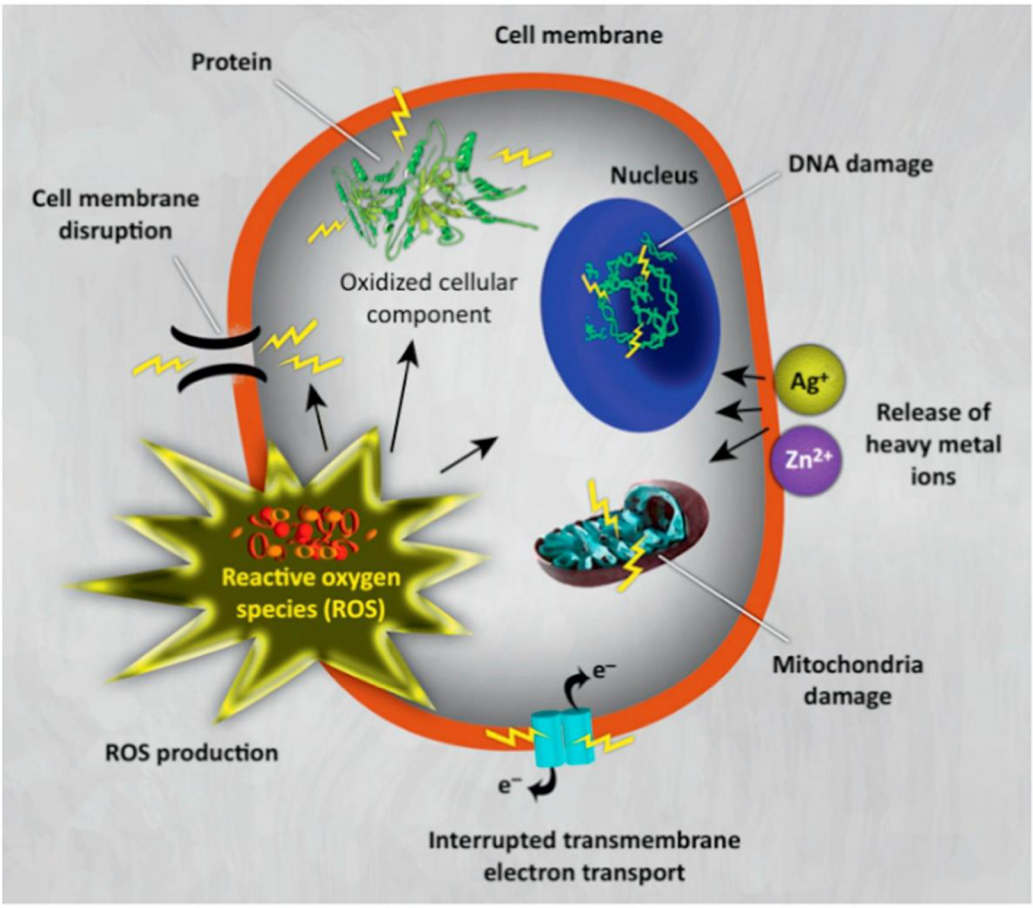

Figure 6: Mechanism of antimicrobial effect of metal nanoparticles [36].

3.4 Immobilization of nanoparticles on polymers

One of the very promising option how to immobilize NPs on polymer membranes is plasma treatment of polymers and subsequent immobilization of NPs on the surface without using any aggressive chemical compounds [60, 61].

Plasma modification usually possess low exposure time (from 5 s to 5 min.). Recently, this approach has been reported as a very successful way how to modify polymers [62, 63]. Plasma treatment is capable to alter the surface physical and chemical properties of polymer without changing the bulk properties. In general, plasma modification is utilized to change the surface chemistry of polymer in order to create new functional groups on the surface of the polymer [64]. Plasma treatment of polymer with various gas types (for example oxygen, nitrogen or ammonia plasma) change the surface energy of polymer and highly reactive species stable in vacuum are created. When these reactive species are exposed to various monomers, they create new surface functional groups such as amine, carboxyl or sulfonate [36, 60, 65]. Thus, by choosing a type of monomer, desired functionalities can be incorporated to the surface of the polymer [66].

Subsequently, various materials, such as NPs (or other compounds) can be immobilized via these functional groups [67-69]. Often an etch-step is performed prior to a deposition process, in order to remove weak boundary layers [70], and to produce radical sites on the surface, onto

which the intended coating will be chemically bonded. Commonly used gases for polymers plasma treatment are argon, nitrogen, oxygen, ammonia, hydrogen, water, nitrogen dioxide, carbon dioxide and carbon monoxide [60].

There are few factors, which have impact on efficiency of the whole process: polymer type, plasma type (e.g. gas type), plasma energy, pressure, concentration of monomer, flow rate, and treatment time [64].

The biggest advantages of plasma treatment include following [60]:

1. Plasma treatment does not influence the bulk properties of the polymers.
2. By choosing a type of gas, it is possible to create desired type of chemical modification of polymer surface.
3. Plasma treatment does not require wet chemical techniques; thus, polymers are prevented from swelling and chemical solvents.
4. Plasma treatment provides uniform modification of polymer surface.

There are also some disadvantages that plasma treatment brings [60]:

1. Plasma treatment must be carried out in vacuum, which increases the cost of the whole process.
2. There is no uniform process of plasma treatment for all types of polymers. Parameters of experiment are usually developed for every sample and cannot be adopted for other sample.
3. It is very difficult to affect the amount of functional groups created on the polymer surface.

When plasma treatment of polymers is utilized, there are few ongoing surface reactions: reactions between surface species and reactions between gas molecules and surface species, cross-linking or degradation [65, 71].

These reactions can be used to achieve various purposes such as [60, 66]:

1. **Plasma polymerization** is driven by polymerization of an organic monomer in plasma (for example CH_4, C_3F) to prolong the main chain of the polymer.
2. **Cleaning and etching** are achieved usually by utilization of oxygen and fluorine containing plasmas resulting in removal of various materials from the surface of polymer forming volatile compounds. Oxygen containing plasma removes organic contamination. The difference between cleaning and etching by plasma treatment lies in the amount of materials that are removed from surface (etching usually provides reaction deeper in the polymer).
3. **Graft polymerization** is a process when various monomers are added and polymerized to create side polymer chains. Grafting density and length of grafted chains can be controlled by plasma parameters including power, pressure and sample disposition, and polymerization conditions such as monomer concentration and grafting time.

Many publications have been dedicated to plasma treatment of polymer with subsequent immobilization of various types of NPs to provide antimicrobial properties [33, 61].

Jiang et al. worked on immobilization of Ag NPs via aldehyde functionalized silicone rubber, stainless steel and paper surfaces. Formaldehyde groups were incorporated using radio frequency-plasma treatment on all types of substrates. Ag NPs were deposited after plasma

treatment via Tollen´s method. They used SEM, atomic force microscopy (AFM) and XRD to investigate and confirm the presence of Ag NPs layer. Aldehyde functional groups were deposited via plasma treatment as follows: base pressure ≈ 6.7 Pa, formaldehyde pressure of ≈ 19.9 Pa, plasma ≈ 33.3 Pa, RF power of 50-150 W, reaction time from 5 s to 2 min, temperature of 170 ºC. Antimicrobial activity of as prepared samples was tested against *Listeria monocytogenes*. These surfaces were exhibited to microbial culture for 24 h. No viable bacteria were detected after 18 and 24 h [72].

Airoudj et al. demonstrated a method for Ag NPs immobilization on cotton fabrics. At first, cotton fabric was functionalized by with maleic anhydride plasma treatment at the pressure of 0.2 mbar and flow rate approximately 1.610^{-9} kg s^{-1}. The power of generator was 30 W. They investigated different deposition times to obtain a thickness of 30 nm. After that, Ag NPs were immobilized by wet chemical reaction. Samples of cotton fabrics were immersed in deionized water for hydrolysis to create carboxylic acid groups and subsequently silver nitrate with concentration of 50 ppm was added to attach the silver ions. Subsequently, Na BH_4 was added for reduction of silver ions to Ag NPs. Surface changes were analyzed by various methods such as SEM and XPS. Presence of Ag NPs was confirmed by UV-VIS spectroscopy and AFM analyses. Size of Ag NPs varied from 5 to 34 nm. Antimicrobial activity of these samples was tested against *E. coli* strain. Cotton samples with immobilized Ag NPs successfully inhibited the growth of bacteria [73].

Hosseini et al. reported on immobilization of Ag NPs on argon plasma treated styrene-butadiene-rubber cation exchange membrane. They investigated the duration of plasma treatment on distribution uniformity of Ag NPs. This experiment resulted in highly uniform distribution of Ag NPs on the membrane sample. They also found out that properties of membrane such as electrical conductivity, flux, current efficiency and ionic permeability were enhanced with the increasing thickness of Ag NPs layer. Energy consumption of flow process decreased [74].

In this thesis, Ag NPs or Se NPs were immobilized on polymer membrane as a prevention from biofouling. Low-pressure plasma with polymerization of cyclopropylamine (CPA) and reactive ion etching (RIE) with ammonia plasma were used to incorporate amine functional groups on polymer membranes. These functional groups enabled further immobilization of both types of NPs (see **Chyba! Nenalezen zdroj odkazů.**). Ag NPs prepared in this work were stabilized w ith sodium citrate. Sodium citrate has three carboxylic acid functional groups, which have solid reactivity with amine groups [75, 76]. Se NPs were stabilized with polyvinylpyrrolidone (PVP). This compound has an amide ring with carbonyl group, which has good reactivity with amine groups, as well [77].

4 Experimental

4.1 Synthesis of silver nanoparticles

In this thesis, several approaches were employed to prepare Ag NPs. Ag NPs were synthetized via wet chemical reduction under different conditions such as temperature, duration of reaction, different stabilizers, concentration of reagents or irradiation of reaction mixture with UV light. All samples of Ag NPs were stored in the fridge at the temperature of 5 ºC in the dark vessel. Here is presented synthesis of hydrazine hydrate-reduced Ag NPs prepared under UV-

irradiation. These Ag NPs had suitable long-term stability and synthesis was fast, easy and reproducible.

4.1.1 Hydrazine hydrate-reduced silver nanoparticles

Following type of Ag NPs was prepared according to article published by Guzmán et al. [19] . Silver nitrate was used as a precursor of silver ions, hydrazine hydrate as reducing agent and sodium citrate as stabilizer. The preparation method was modified by employing the UV-irradiation with different wavelengths. It is known that UV-irradiation can significantly affect the final properties of nanoparticles such shape or size [78].

4.1.1.1 The effect of UV-irradiation

Three different samples denoted as A, B and C were prepared by this synthesis. One additional sample denoted as X was prepared and it served as a control with no UV-irradiation applied. Table 3 shows the conditions of preparation procedure for each sample:

Table 3: Synthesis of hydrazine hydrate-reduced of Ag NPs (the effect of UV-irradiation) - concentration of reagents and wavelengths of UV light.

Name of sample	Wavelength (nm)	Silver nitrate (mM)	Sodium citrate (mM)	Hydrazine hydrate (mM)
X	dark	1	2	1
A	366	1	2	1
B	254	1	2	1
C	400	1	2	1

- *Materials:*

Silver nitrate (p.a., PENTA), hydrazine hydrate (p.a., Sigma-Aldrich), sodium citrate dihydrate (p.a., Sigma-Aldrich), deionized water (resistivity of 18.2 MΩ·cm, Milli-Q®). All materials were used as purchased without further purification. All substances were diluted to aqueous solutions using deionized water. Final solutions of colloidal nanoparticles were purified 3x after synthesis by centrifugation at 14 500 rpm (duration of each cleaning cycle was 30 min).

- *UV-source information:*

Three different wavelengths of UV light were used in this preparation procedure, namely, ≈ 254 nm, ≈ 366 nm. Surface power density of these two UV-sources was 5 mW/cm^2. The third irradiation UV- source had the wavelength of ≈ 400 nm. Surface power density of UV-source with wavelength of 400 nm was 6 mW/cm^2.

- *Method:*

Individual samples were irradiated with UV lamp with various wavelengths. A beaker with the solution of silver nitrate was placed on magnetic stirrer at 500 rpm. UV source was placed 5 cm above the top of the beaker. Afterwards, hydrazine hydrate solution and sodium citrate solution were added at the same time to the beaker with solution of silver nitrate. The reaction was held for 20 min at the dark place - the UV-lamp was the only irradiation source and it was irradiating the reaction mixture during entire reaction process. The temperature of the surrounding environment was ≈ 22 °C. The color of reaction mixture changed continuously from the moment of adding the hydrazine hydrate and sodium citrate into the beaker from light

green to dark green in about 1 min. The pH value of all final colloidal Ag NPs samples was ≈ 6.18.

4.2 Cytotoxicity of silver nanoparticles

For determination of hydrazine hydrate-reduced Ag NPs cytotoxicity, colorimetric qualitative MTT assay was provided. Four samples of prepared Ag NPs were tested, namely X (dark), A (UV-254 nm), B (UV-366 nm) and C (UV-400 nm). Concentration of Ag NPs varied from 2.5 µg/ml to 220 µg/ml.

- *Materials:*

Ag NPs (prepared samples X, A, B, C - concentration varied from 2.5 µg/ml to 400 µg/ml), MTT dye (p.a., Sigma-Aldrich), medium Dulbecco´s Modified Essential Medium (DMEM) (p.a., Sigma Aldrich), DMEM medium was enriched by 10 % Fetal Bovine Serum (FBS) and 2 mM L-glutamin, penicilin (100 U/mL) a streptomycin (100 U/mL), solubilization solution (p.a., Sigma Aldrich), phosphate buffer saline (PBS) (p.a., Sigma Aldrich), mouse fibroblasts NIH-3T3 (ECACC, UK).

Ag NPs were dissolved in DMEM medium. All purchased materials were used as purchased without further purification.

- *Method:*

At first, cell culture was mixed with 100 µl of DMEM, placed in the 96-well and incubated for 24 h at 37 ºC in a humidified 5 % CO_2 incubator. Concentration of cell culture in each well was 1×10^4. After that, medium was removed and replaced by Ag NPs dissolved in medium with the volume of 50 µl. Subsequently, as prepared plate was incubated for 4 h and 6 h at the temperature of 37 ºC. After incubation, cells were washed 3x with pre-heated phosphate buffer saline (PBS) to 37 ºC. In the next step, MTT with the volume of 50 µl was added to each well, as well as 100 µl of medium and incubated for another 2 h in CO_2 incubator. In the final step was added 100 µl of solubilization solution to dissolve the formazan and let sit for 24 h. Results were read by measurement of absorbance at wavelength of 570 nm.

4.3 Antimicrobial activity of silver nanoparticles

Three different methods were used to determine the antimicrobial activity of Ag NPs, namely disk-diffusion method, measurement of growth curves and dilution method. Three samples of Ag NPs were tested: A (UV-254 nm), B (UV-366 nm) and C (UV-400 nm). Various concentrations of Ag NPs samples were tested against strains *E. coli* and *S. aureus*.

4.3.1 Growth curves

- *Materials:*

S. aureus (CCM), *E. coli* NCTC (CCM), prepared Ag NPs samples: A (UV-254 nm), B (UV-366 nm), C (UV-400 nm): concentration of Ag NPs varied from 0.31 mg/ml to 2 500 mg/ml, MH medium (Oxoid, UK), deionized water. All materials were used as purchased without further purification.

- *Method:*

This test was provided in 96- well plate. At first, bacterial culture was diluted with MH broth to 0.5 McF (McFarland standards), subsequently to 1:100. Ag NPs were diluted with deionized water to desired concentrations. In the next step, 100 µl of Ag NPs and 100 µl of diluted cell culture were pipetted to each well. As prepared plate was incubated at 37 ºC for 24 h. The absorbance was measured every 30 min.

4.3.2 Dilution method

- *Materials:*

S. aureus (CCM), *E. coli* (CCM), Ag NPs samples: A (UV-255 nm), B (UV-366 nm), C (UV-400 nm): concentration of Ag NPs was 7 mg/l, MH medium (broth and agar) (Oxoid, UK). All purchased materials were used as purchased without further purification.

- *Method:*

MH agar was used as medium. At first MH agar was autoclaved at 50 ºC. Ag NPs were added to fluid agar (final concentration of Ag NPs in agar was 7 mg/l). As prepared agar was transferred to Petri dish and cooled down at room temperature. Cell culture was grown in MH broth in 24 h and was diluted to concentration of $\approx 1.5\times10^3$ CFU/ml. Subsequently, grown culture was incubated at 37 ºC for 2 h. 100 µl of cell culture was pippeted on agar plates. In the final step, as prepared Petri dishes were incubated at 37 ºC for 24 h and grown colonies were counted as colony forming units (CFU). Control plates were prepared with the same procedure but without Ag NPs. Samples for testing against *S. aureus* were prepared fin 12 repetitions and samples for testing against *E. coli* were prepared in 11 repetitions for statistical analysis.

4.4 Synthesis of selenium nanoparticles

Se NPs were prepared via several methods. Wet chemical synthesis was employed and various reagents were used. Similarly, as for Ag NPs, final properties of Se NPs can be tailored during the synthesis process, as well. Final colloidal solution of Se NPs were stored in the fridge at the temperature of ≈ 5 ºC. Here is presented synthesis of L-cysteine-reduced Se NPs, as this process was easy, fast and reproducible.

4.4.1 L-cysteine-reduced selenium nanoparticles

Three different samples of Se NPs were prepared via this synthesis, namely A1, A2 and A3. Precursor and reducing agent were always the same for every sample, only the stabilizing agents were changed. Sodium selenite was used as a precursor and L-cysteine as reducing agent. The stabilizing agents were polyvinylpyrrolidone-29 (PVP-29), polyvinylpyrrolidone-40 (PVP-40) and bovine serum albumin (BSA). The following Table 4 shows the overview of chemical composition of prepared samples:

Table 4: Synthesis of L-cysteine-reduced Se NPs - composition of samples and concentration of reagents.

Name of sample	Sodium selenite (mM)	L-cysteine (mM)	Stabilizing agent (mM)
A1	25	25	PVP-29 (**0.1**)
A2	25	25	PVP-40 (**0.1**)
A3	25	25	BSA (**1**)

- *Materials:*

Sodium selenite (p.a., Sigma Aldrich), L-cysteine (p.a., Sigma Aldrich), polyvinylpyrrolidone with average molecular weight of ≈ 29 000 g/mol (p.a., Sigma Aldrich), polyvinylpyrrolidone with average molecular weight of ≈ 40 000 g/mol (p.a., Sigma Aldrich), BSA (p.a., Sigma Aldrich), deionized water (resistivity of 18.2 MΩ·cm, Milli-Q®). All materials were used as purchased without further purification. All substances were diluted to aqueous solutions using deionized water. Final solutions of colloidal nanoparticles were purified 3× after synthesis by centrifugation at 10 000 rpm (duration of each cleaning cycle was 20 min.).

- *Method:*

A beaker with 25 ml of aqueous solution of precursor was placed on a magnetic stirrer with 200 rpm at constant ambient temperature of 22 °C. In the next step, the aqueous solutions of reducing agent and stabilizing agent, both 25 ml, were simultaneously added into the beaker. Reaction time was 10 min. Ruby red color of the reaction mixture pointed to the formation of Se NPs. Value of pH of final colloidal solutions was about ≈ 6.23.

4.5 Cytotoxicity of selenium nanoparticles

Cytotoxicity of Se NPs was determined by methods XTT and DNA cell proliferation assay. Sample A1 (L-cysteine reduced and stabilized with PVP-29) was tested.

Three samples were tested:

- A1 in water (denoted as A1W)
- A1 in medium (denoted as A1M)
- A1 in medium – Se NPs without stabilization compound (denoted as A1-0M and used as control)

Se NPs samples were dissolved in medium or in deionized water. Sample without stabilization agent and sample dissolved in deionized water were used to observe if the stabilization compound or water can affect cytotoxicity of Se NPs.

Tests were performed on 96-well plate in triplets for statistical analysis. Seeding density of fibroblasts was 10^4 in each well. Cells were incubated with different concentrations of Se NPs for 24 h. Cells were harvested by trypsinization with 0.25 % trypsin-EDTA (trypsin-ethylenediaminetetraacetic acid). All tests were performed in duplicates for statistical analysis. Concentration of Se NPs varied from 0.005 mg/ml to 5 mg/ml.

4.5.1 XTT assay

- *Materials:*

NIH/3T3 fibroblasts (p.a., Sigma-Aldrich), medium DMEM enriched with 10 % FBS and 5 % penicillin/streptomycin (50 U/ml and 0.05mg/ml), dye XTT (p.a., Sigma-Aldrich), trypsin-EDTA, PBS (p.a., Sigma Aldrich). All materials were used as purchased without further purification.

- *Method:*

At first chosen density of cells was incubated with 100 µl of DMEM overnight. In the next step medium was replaced with Se NPs of various concentration mixed with 100 µl DMEM. After

incubation of 24 h, this mixture was removed and fibroblasts were purified 3× using pre-heated PBS at 37 °C. Then 100 µl DMEM was mixed with 50 µl of XTT and added to each well to the cell culture. Subsequently as prepared 96-well plate was incubated for 2 h in a CO_2 incubator. In the last step, 100 µl of this solution was pipetted into a new 96- well plate to measure an absorbance at the wavelength of 570 nm.

4.5.2 BrdU proliferation assay

- *Materials:*

NIH/3T3 fibroblasts (p.a., Sigma-Aldrich), medium DMEM enriched with 10 % FBS and 5 % penicillin/streptomycin (50 U/ml and 50 µg/ml), BrdU (p.a., Sigma-Aldrich), trypsin-EDTA, PBS (p.a., Sigma Aldrich). All materials were used as purchased without further purification.

- *Method:*

At first chosen density of cells was incubated with 100 µl of DMEM overnight. Se NPs were dissolved in DMEM and 100 µl of this mixture was added to cell culture (again various concentrations). Fibroblasts were incubated with Se NPs for 24 h at humidified atmosphere at 37 °C. In the next step 10 µl of BrdU solution was added to each well followed by additional incubation for another 2 h. After that, labelling medium was removed and 200 µl of FixDenat solution was added to fix the cells for 30 min. Then, this fixing solution was removed and replaced by 100 µl of BrdU-peroxidase antibody solution and incubated at room temperature for 90 min. Then, the wells were rinsed using buffer solution. In the last step 100 µl of substrate solution was added for 20 min and subsequently was measured absorbance at the wavelength of 370 nm.

4.6 Antimicrobial activity of selenium nanoparticles

Antimicrobial activity of Se NPs was determined by two different methods: MIC and measurement of growth curves. Three samples of Se NPs were tested, namely L-cysteine-reduced Se NPs: A1 (stabilized with PVP-29), A2 (stabilized with PVP-40) and A3 (stabilized with BSA).

4.6.1 Minimum inhibitory concentration

- *Materials:*

S. aureus (CCM), *E. coli* (CCM), MH medium (Oxoid, UK), Se NPs samples A1, A2 and A3 (concentration varied from 0.191 mg/ml to 25.5 mg/ml). All materials were used as purchased without further purification.

- *Method:*

Bacterial cultures were diluted to 0.5 McF, subsequently 1:100 with MH medium. Se NPs were dissolved in MH medium to desired concentrations. Test was provided in 96-wll plate. 75 µl of Se NPs and 75 µl of bacterial culture were pippeted to each well and incubated in O/N atmosphere at 37 ºC for 24 h. In the final step, absorbance at the wavelength of 600 nm was measured.

4.6.2 Growth curves

- *Materials:*

S. aureus (CCM), *E. coli* (CCM), *MRSA* (CCM), MH medium (Oxoid, UK), Se NPs samples A1, A2 and A3 (concentration varied from 0.1 mg/ml to 12.25 mg/ml). All materials were used as purchased without further purification.

- *Method:*

This experiment was provided in 96-well plate. Bacterial cultures were diluted to 0.5 McF, subsequently 1:100 with MH medium. Se NPs were diluted with water to desired concentrations. Se NPs with the volume of 100 µl and bacterial culture with the volume of 100 µl were pipetted into each well. As prepared plate was incubated at 37 ºC for 18 h and absorbance was measured every 30 min.

4.7 Plasma treatment of polymer membranes and immobilization of antimicrobial nanoparticles

Polymer membranes were modified with plasma treatment to incorporate amine functional groups for subsequent immobilization of NPs. Two different methods were employed: low-pressure plasma treatment and reactive ion etching (RIE) with utilization of ammonia plasma. As mentioned earlier in this work, only catex membranes were used for all experiments due better stability to various chemicals. Plasma modified membranes were stored in the freezer at the temperature of −15 ºC, in plastic bag containing silica gel to absorb the humidity.

4.7.1 Low-pressure plasma deposition of amine groups on polymer membrane

- *Materials:*

Cyclopropylamine (CPA) (purity 98 %, Sigma Aldrich), argon (purity of 99.998 %, Messer), glacial acetic acid (p.a., Penta), formic acid (p.a., Penta), polymer membrane (catex membrane, MemBrain ltd.). All materials were used as purchased without further purification.

- *Method:*

Polymer membranes were cut to ≈ (1×1) cm^2. At first, membranes were cleaned by pulsed Ar plasma for 10 min before the deposition process. Deposition of amine groups on membranes was done using capacitively coupled plasma (CCP) employing radio frequency (RF) generator with working frequency of 13.56 MHz. Plasma instrument with base pressure of ≈ 1×10^{-4} Pa was equipped with showerhead for uniform gas delivery. The deposition process with length of 1 h was realized via squared pulsed CPA/Ar plasma at pressure of ≈ 50 Pa with power of ≈ 100 W, while the duty cycle was 33 % at repetition frequency of ≈ 500 Hz. Flow rate of Ar and CPA was ≈ 28 cm^3/min and ≈ 2 cm^3/min, respectively.

4.7.2 Deposition of amine groups by reactive ion etching with ammonia plasma on polymer membranes

- Materials:

Argon (purity of 99.999 %, Linde), ammonia (purity of 99.7 %, SIAD), polymer membrane (catex membrane, MemBrain ltd.). All materials were used as purchased without further purification.

- Method:

Second approach of membrane functionalization was done using RIE instrument, which has similar configuration including CCP and RF generator working at the same frequency. Instrument base pressure was ≈ 5×10^{-5} Pa. Samples were precleaned using Ar plasma for 10 min. Then the deposition was done at pressure of 50 Pa with RF power of 50 W for 30 min. The used working gas was Ar with flow of 10 cm^3/min and NH_3 with flow of 40 cm^3/min. Higher RF power caused membrane damaging caused by plasma thermal exposure even if it was realized at higher working pressure.

4.7.3 Immobilization of nanoparticles on polymer membrane

Immobilization process of NPs was held as wet chemical reaction. Plasma treated membranes were immersed into the reaction mixtures of NPs. Membrane samples were immersed in reaction mixtures for 1 h. Subsequently dried for 24 h at the room temperature. As prepared membranes were stored in the dry box. These samples were stored in the dry box for 1 month to reduce the humidity to maximum because of subsequent optical measurements.

Table 5: Polymer membranes samples with immobilized NPs for macro dilution method.

Sample name	Plasma type	Reaction mixture
M1	Low-pressure plasma	Silver nitrate
M2	Low-pressure plasma	Hydrazine hydrate-reduced Ag NPs
M3	Low-pressure plasma	Hydrazine hydrate-reduced Ag NPs stabilized with sodium citrate
M4	Low-pressure plasma	L-cysteine-reduced Se NPs stabilized with PVP-29
MA1	RIE	Silver nitrate
MA2	RIE	Hydrazine hydrate-reduced Ag NPs
MA3	RIE	Hydrazine hydrate-reduced Ag NPs stabilized with sodium citrate
MA4	RIE	L-cysteine-reduced Se NPs stabilized with PVP-29

4.8 Antimicrobial properties of polymer membranes with immobilized nanoparticles

Antimicrobial properties with immobilized NPs (Ag and Se) were tested against cell cultures *S. aureus* and *E. coli* using macro dilution method.

- *Materials:*

S. aureus (CCM), *E. coli* (CCM), MH broth (Oxoid, UK), catex polymer membranes with immobilized NPs. All materials were used as purchased without further purification.

- *Methods:*

Macro dilution method was used to determine the antimicrobial activity of polymer membranes with immobilized NPs. Bacterial cultures were diluted to concentration of 0.5 McF, subsequently to 1:100 with MH broth. Experiment was performed in test tubes and each tube contained with 1 ml of diluted culture. Polymer membrane with the dimensions of ≈ (0.5×0.5) cm^2 were immersed in this solution. Samples were incubated for 24 h at the temperature of 37 ºC. Absorbance was measured at the beginning of the experiment (after

immersing of polymer membrane with immobilized NPs in the medium), after 7 h and after 24 h.

5 Results and discussion

This chapter consists of discussion of achieved results. Sub chapters are in the same order as aim of thesis: synthesis of NPs, cytotoxicity assays, antimicrobial activity of NPs, plasma treatment of polymer membranes with immobilization of NPs and antimicrobial activity of polymer membranes with immobilized NPs.

5.1 Characterization of silver nanoparticles

5.1.1 Hydrazine hydrate-reduced silver nanoparticles

This synthesis employed hydrazine hydrate as a reducing agent, silver nitrate as precursor and sodium citrate stabilizer. This synthesis was with utilization of UV-irradiation with different wavelengths.

5.1.1.1 The effect of UV-irradiation

Figure 7 shows SEM analysis of sample X and TEM analysis of samples A, B and C.

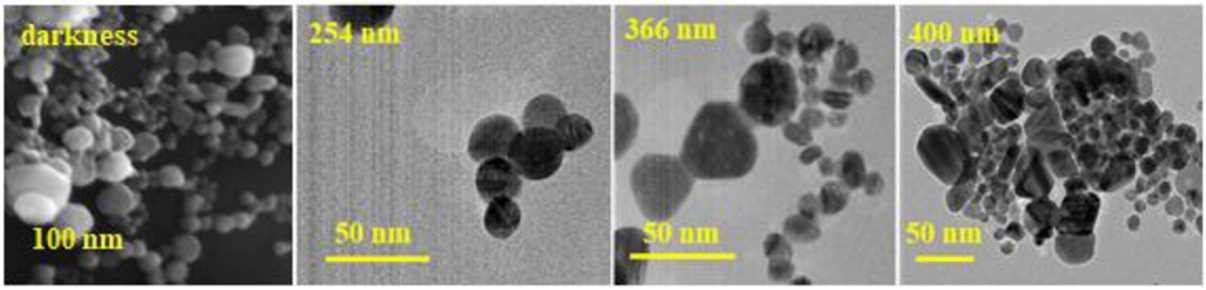

Figure 7: SEM and TEM images of hydrazine hydrate-reduced Ag NPs (the effect of UV-irradiation), from the left: samples X (SEM), A (TEM), B (TEM), C (TEM).

Sample X - darkness: As can be seen on SEM image (Figure 7- left), Ag NPs prepared in dark environment have spherical shape. Size distribution is very wide and ranges from 10 nm to 150 nm.

Sample A - wavelength of 254 nm: Ag NPs irradiated with the UV-source with wavelength of 254 nm are small, up to 50 nm (Figure 7- second from the left). Agglomeration is also visible. In comparison to previous sample X, size of Ag NPs decreased. It is probably caused by the UV-irradiation, which gives additional energy to the reaction system.

Sample B - wavelength of 366 nm: These Ag NPs were irradiated with wavelength of 366 nm (Figure 7– second from the right). Ag NPs. Morphology of these Ag NPs changed visibly. There is a mixture of smaller particles with spherical shape but also bigger particles with anisotropic shape are observable. Ag NPs are grown together. Size distribution is wide and ranges from 10 nm to 50 nm.

Sample C - wavelength of 400 nm: Last sample of Ag NPs was irradiated with the UV- lamp with wavelength of 400 nm Figure 7 - right). Ag NPs from this sample evince also anisotropic shape (triangles with truncated tops, spheres and also rods). According to the literature, with

longer wavelengths the shape of Ag NPs can turn from spherical to anisotropic [79]. Number of particles with bigger size was increased in comparison to sample B. Size of Ag NPs vary from 10 nm to 50 nm. Agglomeration is visible.

All samples have typical absorption maximum of SPR at the wavelength of 420 nm. Sample X evince the highest intensity of absorption peak of all samples, probably due to big particles. The absorption spectra of samples A and B are very similar with little difference that sample A shows higher intensity of SPR, which can be caused by smaller particles present in the solution as confirmed by SEM and TEM. Absorption spectrum of sample C is different, it has the highest intensity of UV-irradiated samples and exhibits also secondary absorption peak at higher wavelengths which is probably caused by bigger size of Ag NPs and also their anisotropic shape. Absorption spectra of samples X, A, B and C are shown in Figure 8.

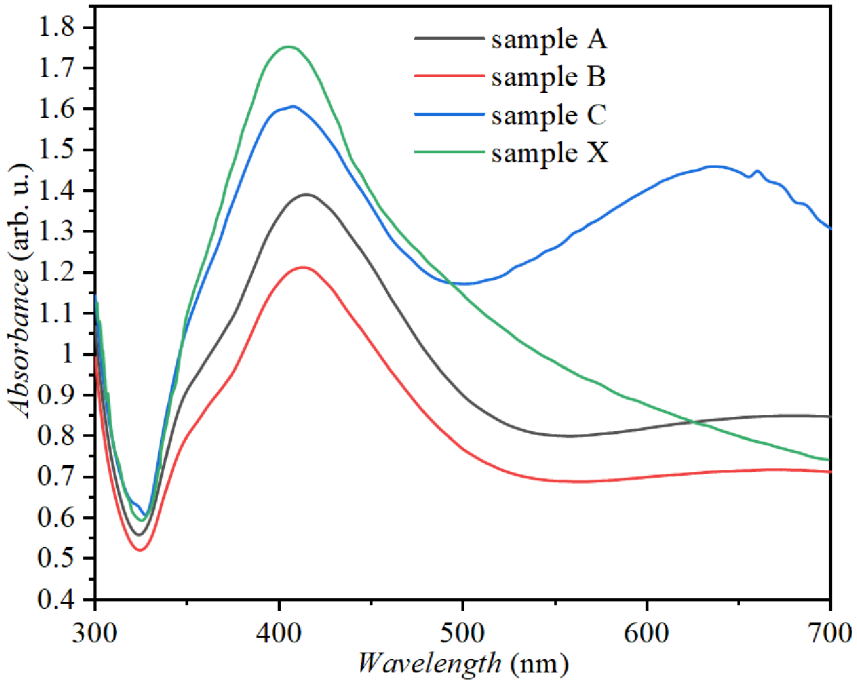

Figure 8: Absorption spectra of hydrazine hydrate-reduced Ag NPs (the effect of UV-irradiation): samples A (UV-254 nm), B (UV-366 nm), C (UV-400 nm) and X (darkness).

Stability of as prepared Ag NPs was measured within 3 weeks by UV-VIS absorption spectrometry (see Figure 9). Stability of samples A, B and C lasted for 3 weeks. Sample X was stable for ≈ 7 days after preparation procedure. After this period, agglomerates could be seen at the bottom of the flask. Thus, long-term stability of this sample was not measured.

These experiments showed that UV-irradiation has significant effect on final properties of Ag NPs. Most significant changes appeared for shape and size of Ag NPs. With increasing wavelength of UV-irradiation, the shape of Ag NPs turned from spherical to anisotropic. UV-irradiation gives additional energy to the reaction mixture. The size of Ag NPs increased, as well. These particles were stable for 3 weeks as confirmed the UV-VIS spectrometry. After this period, sediments were seen at the bottom of the flask. Thanks to the stability of weeks, Ag NPs were sufficient for other experiments.

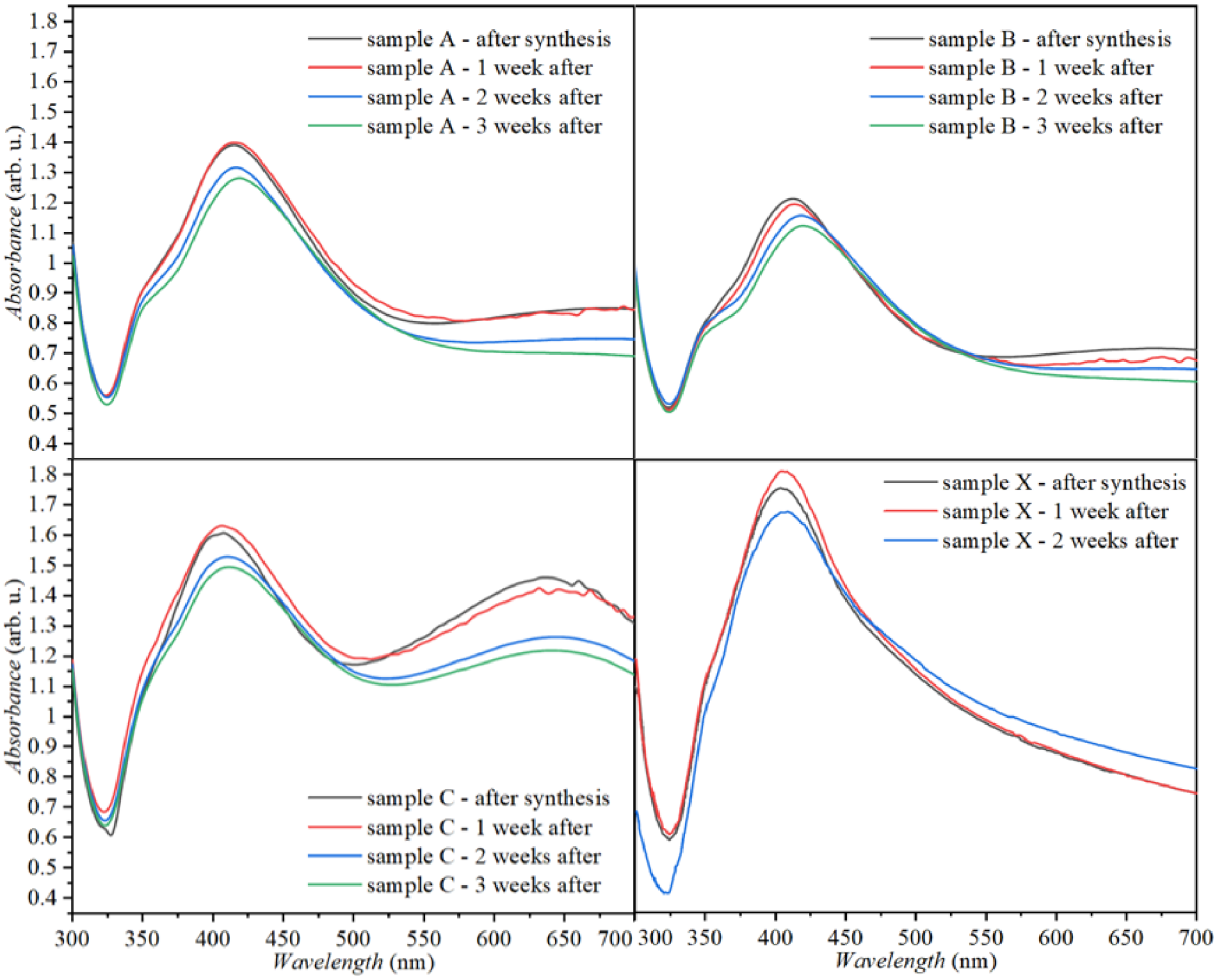

Figure 9: Stability of hydrazine hydrate-reduced Ag NPs (the effect of UV-irradiation): samples A (UV-254 nm), B (UV-366 nm), C (UV-400 nm) and X (darkness) measured by UV-VIS absorption spectrometry.

5.1.2 Cytotoxicity of silver nanoparticles

Figure 10 shows viability and standard deviation (SD) of MTT cytotoxicity assay of Ag NPs with different concentrations and also incubation time of individual samples that were tested.

Hydrazine hydrate-reduced Ag NPs samples prepared under UV-light: A (UV-254 nm), B (UV-366 nm), C (UV-400 nm) and X (darkness) were tested using MTT assay to determine their cytotoxicity. After the experiment, when Ag NPs were incubated with cell culture, viability of cells was calculated related to concentration of Ag NPs.

However, during this assay, several difficulties occurred. All tested samples of Ag NPs possess high value of measurement error but most significantly sample B. These errors are attributed to very difficult preparation of Ag NPs for this test. MTT assay requires exact concentrations of Ag NPs to determine, which concentration causes cytotoxicity. Thus, Ag NPs were centrifugated at the speed of 14 500 rpm for 1 h and 30 min. After that, supernatant was removed and sediment with particles was placed to a small Petri dish. Subsequently Ag NPs were dried in the oven at 80 °C for 1 h

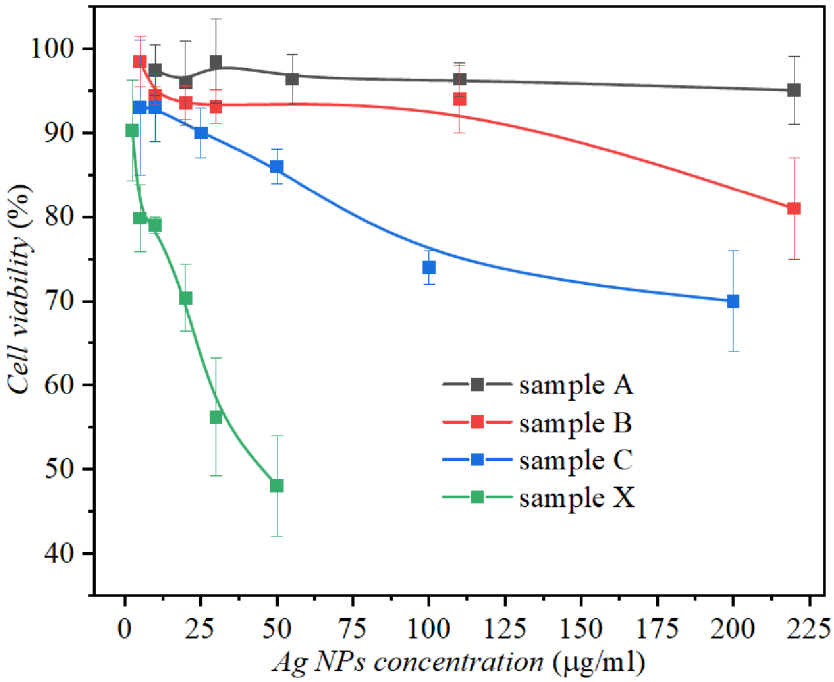

Figure 10: MTT cytotoxicity assay of hydrazine hydrate-reduced Ag NPs prepared with utilization of UV-irradiation - viability of cell culture related to concentration of Ag NPs samples A (UV-254 nm), B (UV-366 nm), C (UV-400 nm) and X (darkness).

. The yield of Ag NPs was very small and it was very difficult to scrub the dried Ag NPs from the Petri dish. Another point, which should be discussed is the drying temperature, which might change the properties of Ag NPs. Another obstacle was stability of Ag NPs. Ag NPs were originally dispersed in deionized water but water is not appropriate medium for cell culture used in this cytotoxicity assay (it can cause lysis or rupture of the cells), thus it could negatively affect not only the cell culture but also the results of the testing. Ag NPs had to be dissolved in DMEM medium but they agglomerated immediately - agglomerates could be seen by eye. Thus, vial with Ag NPs was placed to an ultrasound bath with for 10 min. This procedure helped to disperse the Ag NPs to colloidal solution but only for a limited period of ≈ 24 h. After this time, agglomerates of Ag NPs were visible at the bottom of the vial, again. Additionally, some resulting values of cell viability were excluded because of statistical reasons. Nevertheless, despite that there were issues with Ag NPs preparation and their colloidal stability. All of the samples evince a certain trend of cell mortality with increasing concentration. Graph also shows that viability of cell culture was only ≈ 90 % at the beginning of the test for sample X and for sample C. In this case it cannot be stated that decrease of cell viability is caused only by Ag NPs.

Cell viability can be affected by many factors such as sterility of environment, incubation conditions, medium content etc. It points to that also a human factor needs to be considered when error measurement is provided.

5.1.3 Antimicrobial activity of silver nanoparticles

Three antimicrobial methods were employed to determine the antimicrobial properties of hydrazine hydrate-reduce Ag NPs: disk-diffusion method, measurement of growth curves and dilution method with subsequent counting of grown colonies. Three samples prepared under UV-irradiation were used, namely A (UV-254 nm), B (UV-366 nm) and C (UV-400 nm). Ag NPs were tested against strains *S. aureus* and *E. coli*. In this shorten thesis only growth curves and dilution methods are presented. Growth curves of several samples and dilution method are presented as these methods showed relevant results.

5.1.3.1 Growth curves

Figure 11 show results from the measurement of growth curves with applied Ag NPs. Only sample A (UV-254 nm) and sample C (UV-400 nm) are presented as they showed relevant results.

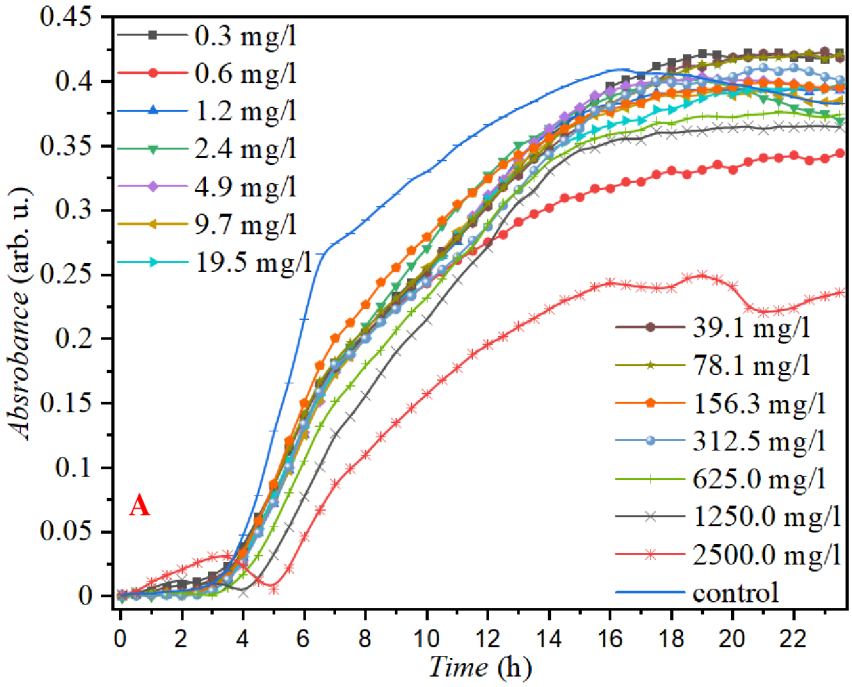

Figure 11: Growth curves of S. aureus with applied hydrazine hydrate-reduced Ag NPs prepared under UV-irradiation: sample A (UV-254 nm).

Ag NPs were applied with various concentrations to determine, which one of them can suppress or affect the growth of the cell cultures. Concentration of Ag NPs varied from 0.31 mg/ml to 2 500 mg/ml. The highest concentration of 2 500 mg/ml showed partial suppression of cell growth for all applied samples, where the cell culture did not grow to the maximum values as a control (control was only bacterial culture without Ag NPs). The most significant inhibition of growth is visible for sample A. Unfortunately, results are not significant and antimicrobial effect of Ag NPs could not be confirmed. This can by caused by fact, that the concentration of Ag NPs is too low or that Ag NPs are not effective against strain *S. aureus*. Dark color of colloidal solutions with higher concentrations could also decreases spectroscopy analysis accuracy.

The same experiment was provided for strain *E. coli.* Figure 12 shows results from measuring growth curves of *E. coli* with applied concentrations of Ag NPs. As in previous case, fourteen different concentrations of Ag NPs were applied (from 0.31 mg/ml to 2 500 mg/ml). The highest concentration of 2 500 mg/ml showed partial suppression of bacterial culture for all samples. The most significant result was observable for sample C, where the growth of cell culture was successfully stopped. However, this result could be affected by dark color of the colloidal solution and could cause issues during spectroscopy reading.

This method showed that several concentrations of Ag NPs can suppress the growth of bacterial cell culture or even stop the growth. However, results from testing Ag NPs against *S. aureus* were not significant and spectroscopy reading could be affected by dark color of the colloidal solutions of Ag NPs (especially at higher concentrations). Thus, another test was provided to confirm the antimicrobial properties of Ag NPs, where spectroscopy measurement is not necessary to determine the results.

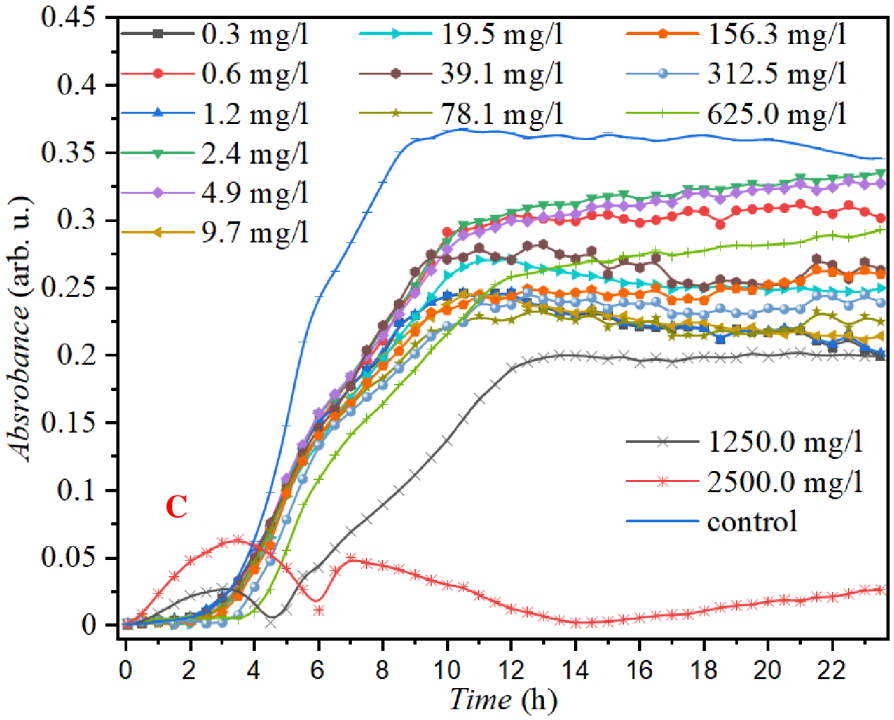

Figure 12: Growth curves of E. coli with applied hydrazine hydrate-reduced Ag NPs prepared under UV-irradiation: sample C (UV-400 nm).

5.1.3.2 Dilution method

Dilution method was employed to determine the antimicrobial properties of Ag NPs, where Ag NPs were added directly to the medium and cell culture was let to grow in such prepared medium. Grown colonies were manually counted in the final step. *Figure 13* shows results from testing Ag NPs against *S. aureus.* This test determines how effectively Ag NPs can prevent cell culture from growing. As results showed, samples A and C seem to be the most effective. They were able to stop the growth of *S. aureus* almost of 50 %. Unfortunately, sample B did not prevent cell culture from growing (only very slightly).

An interesting result was investigated for sample B, where the antimicrobial functionality occurred only minimally against *S. aureus* and for strain *E. coli* the growth of the bacterial culture even increased in comparison to the control. However, a correlation can be found between antimicrobial action and the size and shape of Ag NPs. As mentioned several times in this work, particle size plays an important role. The smaller is the particle, the larger antimicrobial effect should occur. As we can see, samples A and C proved to be the most effective. We know from the characterization of these particles that sample A have small, mostly spherical particles with a size of about 50 nm and sample C is a mix of smaller particles (spherical) with larger particles (various shapes - spheres, rods, plate triangles with truncated tops). Therefore, the size and shape of Ag NPs also plays a role in this case. As for the culture of *E. coli*, Graves et al. published an article stating that *E. coli* is able to develop resistance against Ag NPs very quickly. This is due to the fact that the use of Ag NPs in the commercial sphere has rapidly increased in recent years (for example in cosmetics) [80].

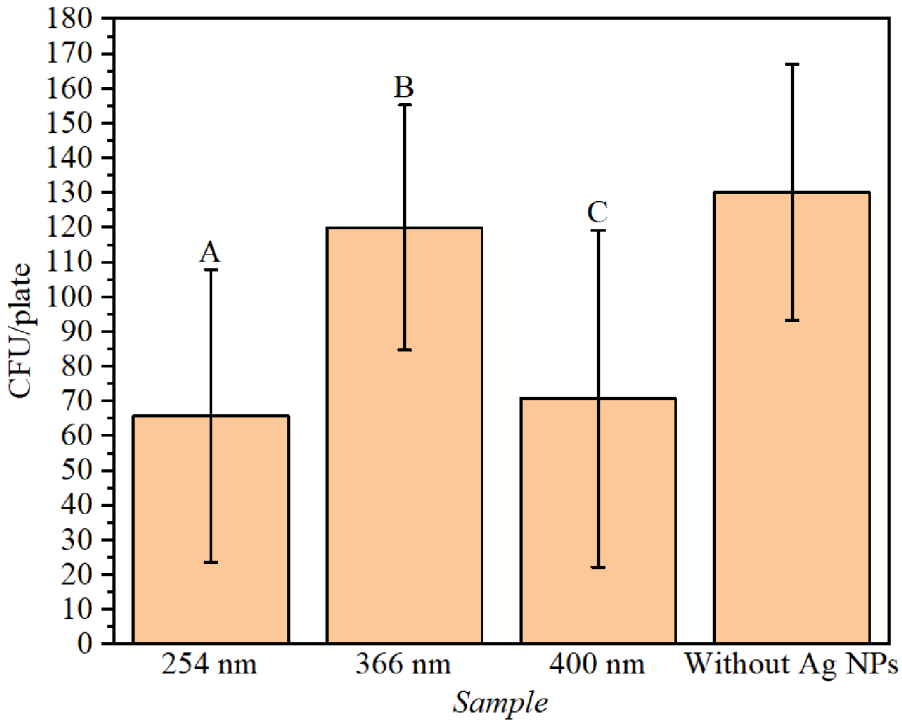

Figure 13: Colony forming units of S. aureus with applied hydrazine hydrate-reduced Ag NPs prepared under UV-irradiation: samples A, B and C

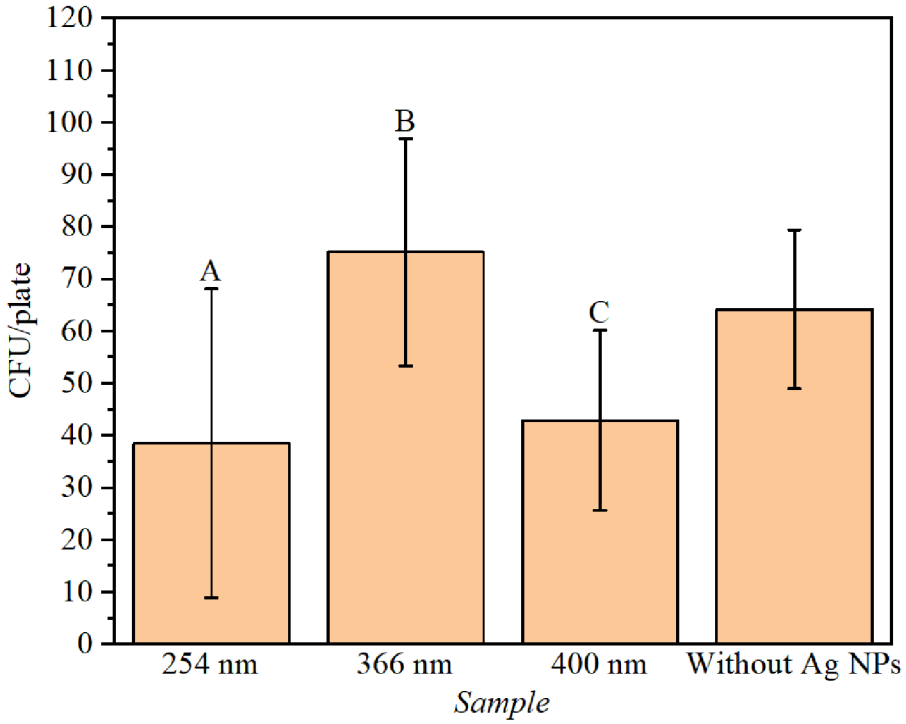

Figure 14: Colony forming units of E. coli with applied hydrazine hydrate-reduced Ag NPs prepared under UV-irradiation: samples A, B and C.

5.2 Characterization of selenium nanoparticles

5.2.1 L-cysteine-reduced selenium nanoparticles

In order to characterize the morphology and size of Se NPs, STEM analysis was performed. Figure 15 shows STEM images of sample A1 with two different magnifications with corresponding view fields of ≈ 3.45 µm (left) and ≈ 1.65 µm (right), respectively, where the PVP-29 was used as a stabilizing agent. The Se NPs do not tend to form agglomerates and they are well separated and spherically shaped. A dominant size of Se NPs is ≈ 40 nm, however the size distribution is not monodispersed.

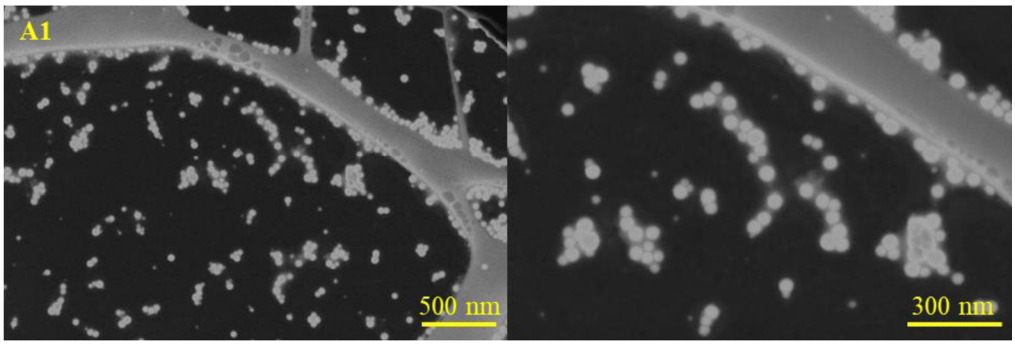

Figure 15: STEM image of L-cysteine-reduced Se NPs - sample A1 (stabilized with PVP-29).

Figure 16 shows STEM images of sample A2 with two different magnifications with corresponding view fields of 3.45 μm (left) and 1.65 μm (right), respectively, where the PVP-40 was used as a stabilizing agent. The shape of Se NPs is also spherical. A thin stabilizing layer of PVP-40 can be clearly seen on an individual particle as a white outer circle. A dominant size of Se NPs is the around ≈ 50 nm. It is obvious that size distribution of Se NPs is more monodisperse than in the sample A1.

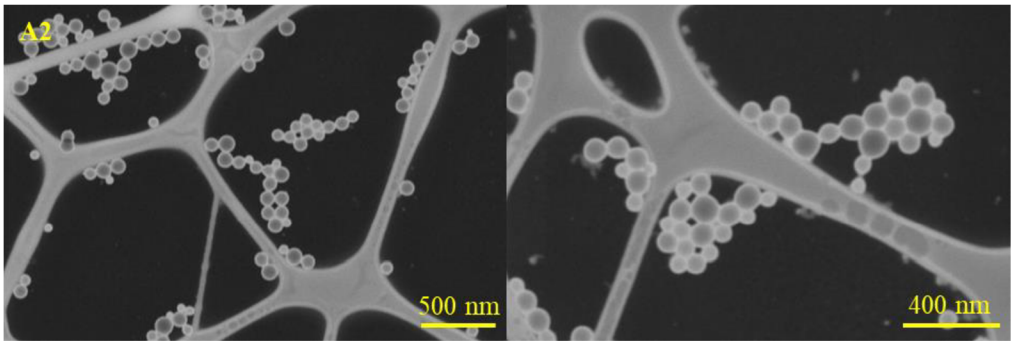

Figure 16: STEM image of L-cysteine-reduced Se NPs - sample A2 (stabilized with PVP-40).

Figure 17 shows STEM images of sample A3 with two different magnifications with corresponding view fields of 3.45 μm (left) and 1.65 μm (right), respectively, where the BSA was used as stabilizing agent. Formed Se NPs are separated and spherically shaped. Size distribution of Se NPs is highly polydispersed and size varies from 50 nm to 100 nm.

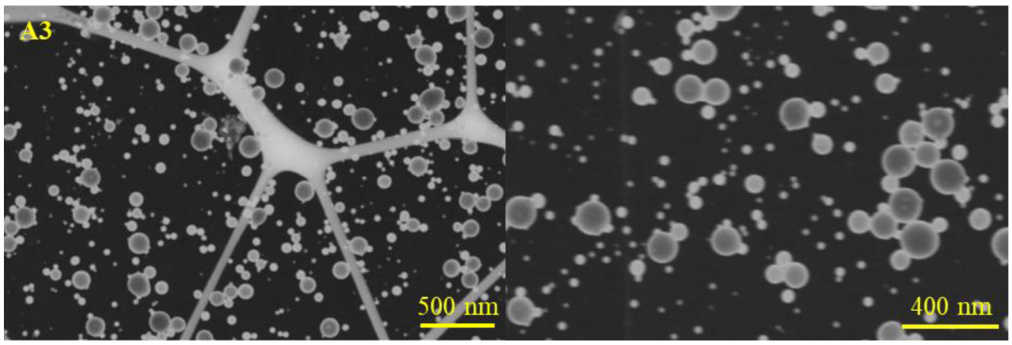

Figure 17: STEM image of L-cysteine-reduced Se NPs - sample A3 (stabilized with BSA).

Figure 18 shows UV-VIS spectroscopy of as prepared L-cysteine-reduced Se NPs. The color of all reaction mixtures changed into ruby red after ≈ 2 min. This change visually pointed to the

formation of Se NPs. This analysis revealed that absorption maximum of Se NPs samples A1 and A2 is at the wavelength of 275 nm. Absorption maximum of Se NPs sample A3 is at 265 nm. As can be seen, sample A3 has a slightly shifted peak of absorption maxima, probably due to a different stabilizer in comparison to A1 (stabilized with PVP-29) and to sample A2 (stabilized with PVP-40). M

The antimicrobial activity is very significantly affected by the size of particles, the smaller is the nanoparticle, the higher is the antimicrobial effect. Following this rule, sample A1 was found as a most suitable for immobilization on polymer membrane because of the smallest size among all prepared samples.

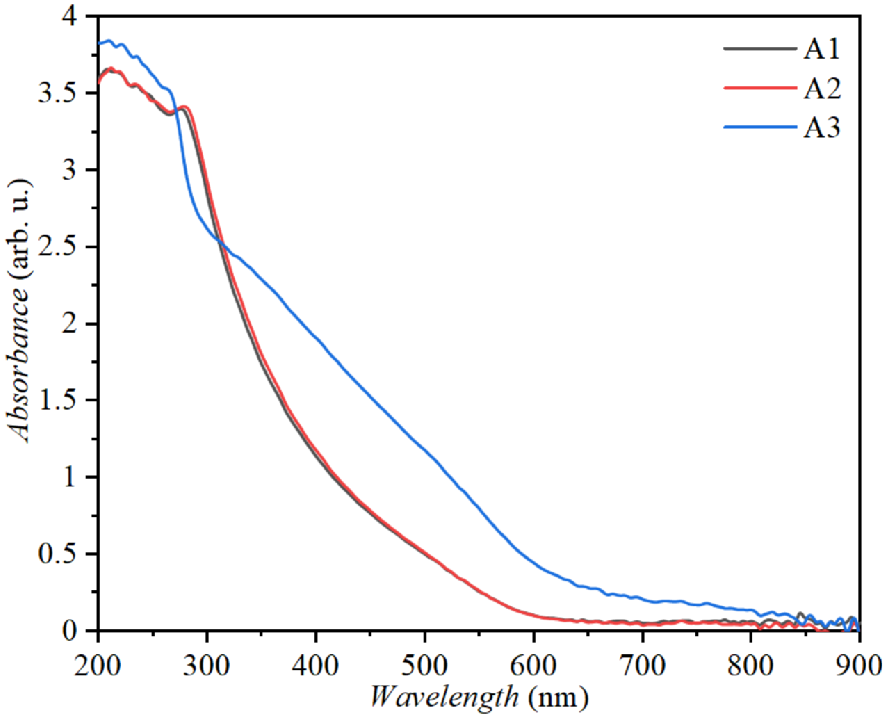

Figure 18: Absorption spectra of L-cysteine-reduced Se NPs - sample A1 (stabilized with PVP-29), A2 (stabilized with PVP-40) and A3 (stabilized with BSA).

5.2.2 Cytotoxicity of selenium nanoparticles

XTT is qualitative assay and represents metabolic activity of the cell and can be related to viability of cells, under defined conditions. Metabolic activity of cells is given by mitochondrial activity, where cells produces NAD(P)H-dependent oxidoreductase enzymes, which can reduce the tetrazolium dye (XTT dye) to orange formazan [81]. In general, the darker is the resulting solution, the higher is the metabolic activity of the cell. Thus, the higher is the metabolic activity, the number of viable cells should be higher, as well. On the other hand, there is DNA cell proliferation assay, which is a quantitative analysis and reflects the proliferation of the cells. It should be noted that not all cells that are divided can survive, but still can contain BrdU. Additionally, metabolic activity is driven by several factors, not only from mitochondrial activity but also from cell proliferation rate, cell size, metabolic rate and cell survival. However, these two types of tests should not be compared because they represent different mechanisms in the cell [82]. L-cysteine-reduced Se NPs were tested (sample A1). This sample was stabilized

with PVP-29 and few factors were investigated, namely Se NPs in water (sample A1W), Se NPs in medium (A1M) and Se NPs without stabilization layer dispersed in medium (A1-0M).

Thus, when cytotoxicity of various compounds is considered, in this case Se NPs, cytotoxicity can be caused by several factors, as well (metabolic activity, cell proliferation, mRNA yield, etc.). As can be seen from performed XTT assay (see Figure 19) and DNA cell proliferation assay (see Figure 20), Se NPs might be causing cytotoxic effect at higher concentrations (2 mg/l and 5 mg/l). To be more detailed, XTT test showed that Se NPs at lower concentrations can increase the metabolic activity. Se is a micronutrient and at very low concentrations, it can enhance several cell mechanisms such as metabolic activity. On the other hand, high concentration of Se NPs might have an impact on cell mechanisms such as decrease of metabolic activity or even cause cytotoxicity (cell death). This corresponds to well-known hormetic effect of Se, i.e. positive influence at adequate dose and negative at high dose [83]. As the XTT graph shows, metabolic activity decreased very significantly with increasing concentration of Se NPs (2 mg/l and 5 mg/l). DNA proliferation assay showed similar information about the concentration of Se NPs, even if it represents different mechanisms in cell. With lower concentrations, the proliferation of cells increased, but with increasing concentration of Se NPs, cell proliferation rapidly decreased. Thus, both of these tests showed that with very low concentration of Se NPs some of the mechanisms of cells can be supported even enhanced but with high concentrations of Se NPs, these mechanisms can decrease very rapidly.

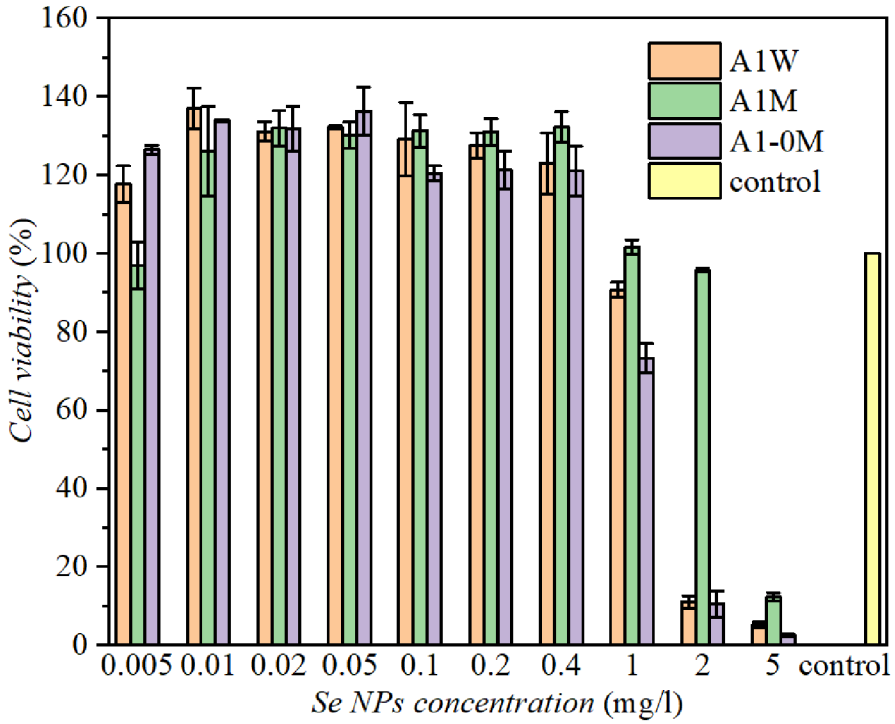

Figure 19: Results of XTT assay with applied concentrations of L-cysteine-reduced Se NPs.

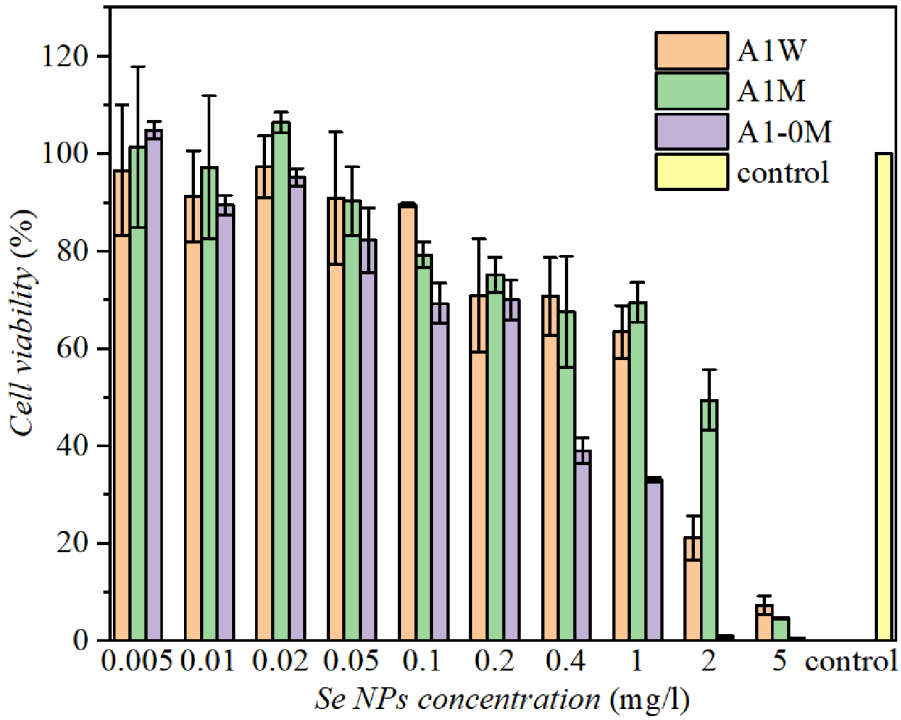

Figure 20:Results of BrdU cell proliferation assay with applied concentrations of L-cysteine-reduced Se NPs.

5.2.3 Antimicrobial activity of selenium nanoparticles

Antimicrobial activity of L-cysteine-reduced Se NPs was tested with two methods: MIC and measurement of growth curves. Three samples were tested, sample A1 (stabilized with PVP-29), A2 (stabilized with PVP-40) and A3 (stabilized with BSA). Influence of few factors were investigated: size and size distribution and also different stabilizing agents. Concentration of Se NPs varied from 0.096 mg/ml to 12.25 mg/ml.

5.2.3.1 Minimum inhibitory concentration

Figure 21 shows results from testing Se NPs against strain *E. coli*. It is obvious that all three samples of Se NPs (A1, A2 and A3) show very similar effect on this bacterial culture. In this case, it also appears that increasing or decreasing concentrations of Se NPs did not have any significant effect on the growth of the bacterial culture. *E. coli* growth was suppressed only partially. Se NPs suppressed the growth of bacterial culture by approximately of 20-30 %. As no MIC has been determined, this indicates, that these Se NPs evince bacteriostatic rather than bactericidal properties. There is also a possibility that the Se NPs concentration was too low to stop the growth of the bacterial culture. It can be also assumed that as in the above-mentioned tests of Ag NPs, it can be assumed that *E. coli* is able to develop antimicrobial resistance very quickly. Therefore, it was not possible to unambiguously determine the antimicrobial properties of nanoparticles with this test. Thus, another method was used to gain more information about Se NPs antimicrobial properties.

The MIC test of all three Se NPs samples was also performed for *S. aureus* bacterial culture shown in Figure 22. For sample A1, the concentration of 0.096 mg/ml appeared to be the most

effective, however, the growth of bacteria was not stopped completely. Sample A2 slowed the growth of the bacteria very slightly. Sample A3 stopped the growth of *S. aureus* by approximately 50 % with the concentration of 0.191 mg/ml. However, an interesting phenomenon was observed - with increasing concentration of Se NPs, bacterial growth increased rather than decreased.

These set of experiments have shown that L-cysteine-reduced Se NPs samples evinced only partial antimicrobial activity against both of the cell cultures. Unfortunately, it was not possible to determine a MIC in the tests applied for *E. coli* and *S. aureus*, as none of the chosen concentrations stopped the growth of the bacteria. However, at higher concentrations the growth of bacteria stopped only partially or not at all. This fact is interesting because scientific publications mostly state that the antimicrobial effect of Se NPs increases with increasing concentration. As can be seen, there are also differences between samples. It seems that, in case of testing Se NPs against *E. coli*, the size distribution or stabilizer does not have any significant effect on final antimicrobial properties. However, in case of testing Se NPs against *S. aureus*, there are several differences between samples. It seems that sample A1 (stabilized with PVP-29) evinced the strongest antimicrobial effect at most of the chosen concentrations (except of the 0.38 mg/l, 1.53 mg/l and 12.25 mg/ml). Sample A2 (stabilized with PVP-40) seems to evince the lowest efficacy of antimicrobial properties. Sample A3 (stabilized with BSA) was most effective at the lowest concentrations. It seems that size of Se NPs and also their stabilization layer, can have potential influence on the final antimicrobial properties of Se NPs and it also shows different reactivity to Gram-positive or Gram-negative bacteria. However, another type of antimicrobial testing was performed for comparison, especially to examine above mentioned phenomenon (see following chapter).

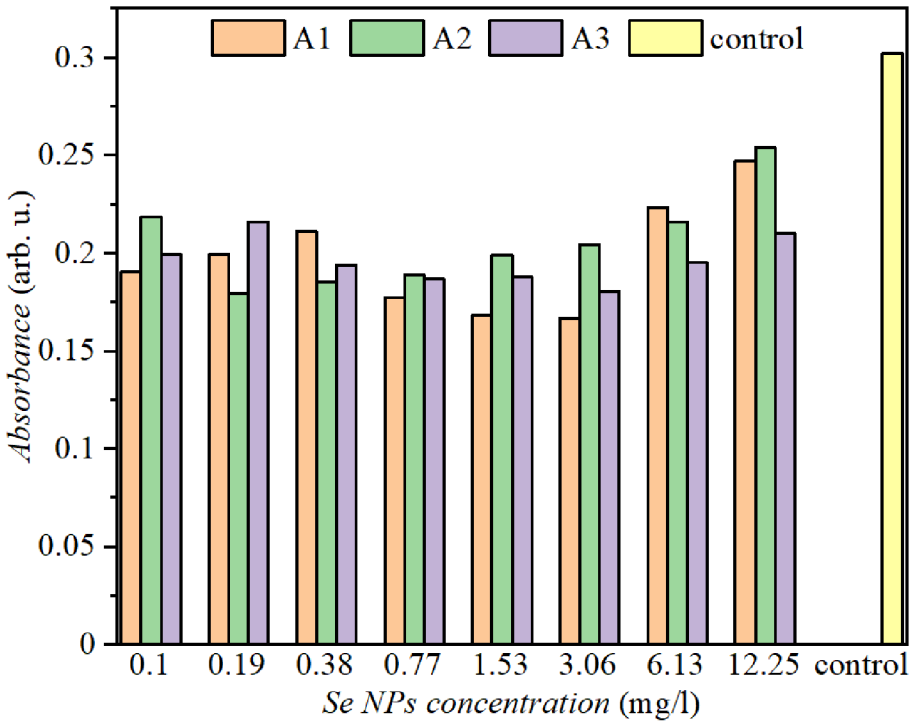

Figure 21: MIC results of L-cysteine-reduced Se NPs applied against E. coli: sample A1 (stabilized with PVP-29), sample A2 (stabilized with PVP-40) and sample A3 (stabilized with BSA).

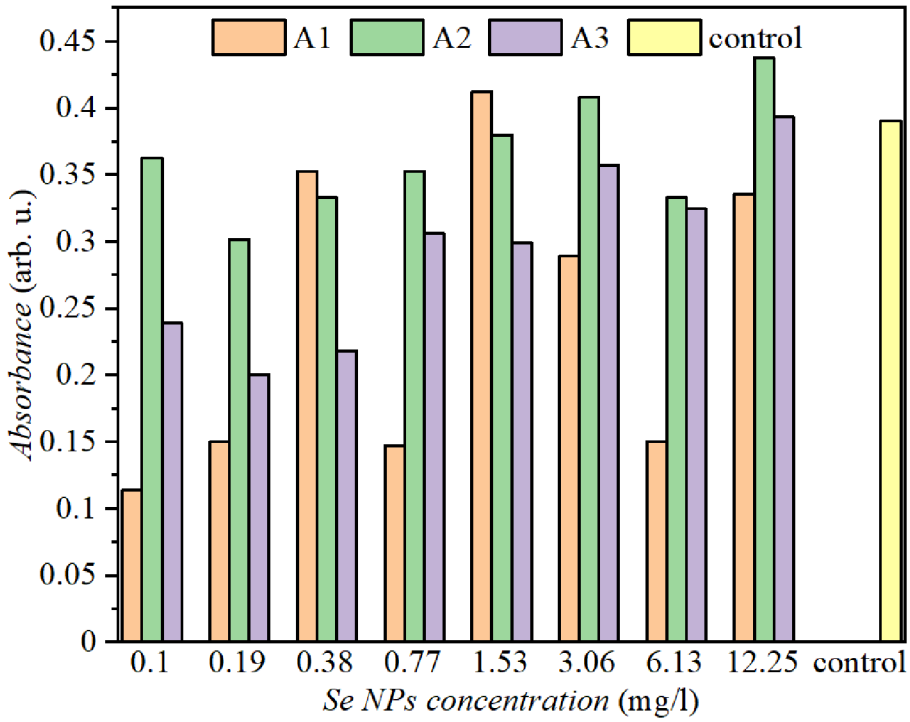

Figure 22: MIC results of L-cysteine-reduced Se NPs applied against S. aureus: sample A1 (stabilized with PVP-29), sample A2 (stabilized with PVP-40) and sample A3 (stabilized with BSA)

5.2.3.2 Growth curves

Measurement of growth curves was also provided on bacterial strain *S. aureus*. on all three L-cysteine reduced Se NPs: A1 stabilized with PVP-29, sample A2 stabilized with PVP-40, sample A3 stabilized with BSA. Only sample A is presented, as the results for remaining samples A2 and A3 were similar.

Figure 23 shows that sample A1 effectively suppressed the growth of bacterial culture at the lowest concentrations (from 0.096 mg/ml to 0.766 mg/ml). With increasing concentration of Se NPs, the lag phase of the growth curve was significantly prolonged. This effect was also observed for the remaining two samples A2 and A3. The prolonged lag phase could indicate a bacteriostatic effect of Se NPs.

The other bacterial culture with applied Se NPs, where growth curves were measured, was *E. coli*. Figure 24 shows results of this measurement for sample A1. The results show that the growth of bacterial strain *E. coli* was affected only slightly. It can be also seen that the concentration of Se NPs did not affect the growth of the bacterial culture. This result correlates with the result from a previous MIC measurement test, where it was also shown that any selected concentration of Se NPs does not affect the growth of *E. coli*. This was observed for all L-cysteine reduced samples (also samples A2 and A3)

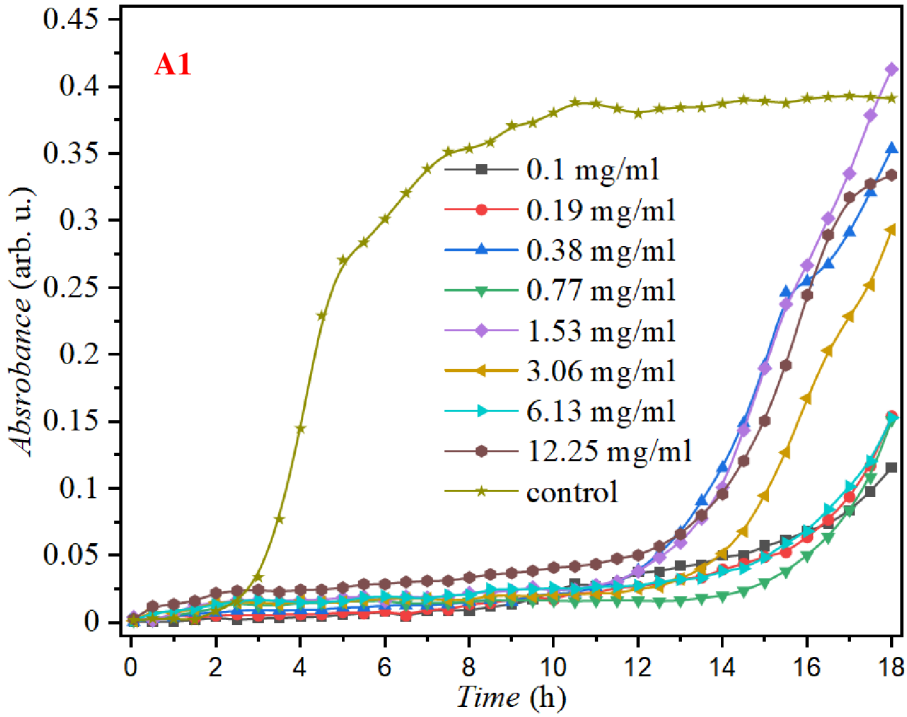

Figure 23: Growth curves of S. aureus with applied L-cysteine-reduced Se NPs: sample A1 (stabilized with PVP-29).

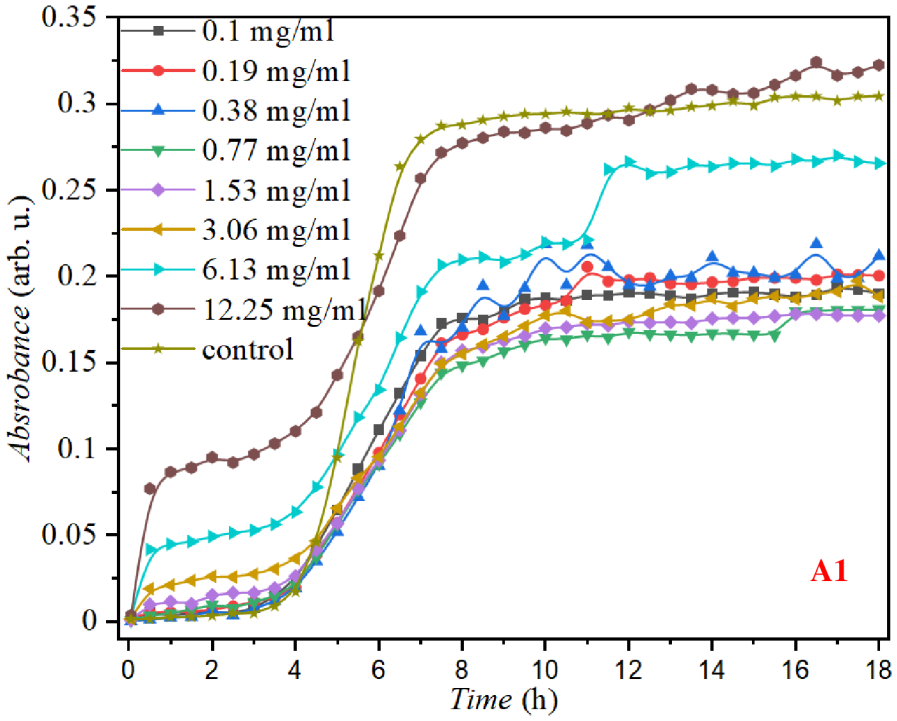

Figure 24: Growth curves of E. coli with applied L-cysteine-reduced Se NPs: samples A1 (stabilized with PVP-29).

Testing on bacterial culture *S. aureus* showed that Se NPs were able to stop the bacterial growth only partially. In this case, these results point to fact, that Se NPs evince more bacteriostatic

rather than a bactericidal effect against *S. aureus* strain. Se NPs have also been tested on bacterial culture. *E. coli*. It was found out, that any concentration of Se NPs (increasing or decreasing) did not affect the growth of the bacteria significantly, which was confirmed as a correlation between MIC testing and measurement of growth curves. The growth of the bacterial culture was suppressed only slightly. In this case, there are several options how results can be understood. Se NPs did not have any antimicrobial properties against *E. coli* bacterial culture. The concentration of Se NPs was not sufficient to affect the growth, possibly, in the same way as for the above-mentioned Ag NPs, *E. coli* is able to very quickly develop the resistance against antimicrobial agent. From these results, it could be stated that Se NPs against *E. coli* show only a partial bacteriostatic effect.

However, an interesting phenomenon has been found during testing of bacterial culture *S. aureus*, which has not been published in any available literature, yet. The results showed that with increasing concentration of Se NPs, the antimicrobial effect decreased. The results from both MIC and growth curves, where the lag phase was significantly prolonged at higher concentrations, correlated. This refers to the fact that Se NPs at higher concentrations act as bacteriostatic rather than bactericidal compound. This fact is interesting mainly because most available scientific publications state that the antimicrobial effect also increases with increasing concentration of antimicrobial compound [84].

5.3 Plasma treatment of polymer membranes and immobilization of nanoparticles

Due to the composition of polymer membrane, its plasma treatment was complicated. The first issue was related to the process of deposition of amine groups in a vacuum. Since the membrane started to release a big amount of gas, it was necessary to pump the chamber for a very long time. After deposition of the amine groups, it was necessary to immobilize the antimicrobial NPs on the membrane in very short time. The longer the membrane would stand, the more the stability of the deposited groups would decrease due to binding of oxygen, humidity, etc.

In addition, the immobilization process was carried out as a wet chemical reaction, which causes the swelling of the membrane. Although the membrane was able to dry, some amount of humidity was still absorbed in it. It should be noted that membranes with deposited amine groups needed to be stored frozen in a refrigerator, ideally with silica gel beads to prevent binding of moisture. Due to the release of gas from the membrane in vacuum, it was necessary to choose a suitable technique to determine the bindings, which were formed between NPs and polymer membrane. Therefore, the analysis was done by Fourier-transform infrared spectroscopy (FTIR), which does not need to be performed in a vacuum.

Another obstacle was the immobilization of Ag NPs on the membrane. The plasma treated membrane with deposited amino groups was immersed in the reaction solution to synthesize Ag NPs directly on the membrane. It was found that all tested wavelengths of UV-irradiation, used for synthesis of hydrazine-hydrate reduced Ag NPs, affected the stability of the membrane and caused its degradation. The membrane began to dissolve and the solution with Ag NPs evinced a strong turbidity. However, it was obvious from provided antimicrobial tests that the composition of Ag NPs (e.g. silver nitrate used as a precursor, hydrazine hydrate as reductant, and sodium citrate as stabilizer) showed at least partial antimicrobial properties (bacteriostatic properties). Therefore, Ag NPs that were immobilized on the membrane were prepared without

UV-irradiation. Under such synthesis condition, it was possible to observe how the individual components of reaction solution affect the final antimicrobial properties of Ag NPs.

5.3.1 Low-pressure plasma deposition of amine groups on polymer membranes

FTIR analysis of low-pressure plasma deposition with polymerization of CPA is shown in Figure 25. According to FTIR spectra of all samples of polymer membranes with immobilized NPs, it can be assumed that combination of various amide groups was present on the membranes with immobilized NPs, namely basic N-H stretching, primary, secondary, and tertiary amides, which have typical peaks at the certain wavenumbers [85].

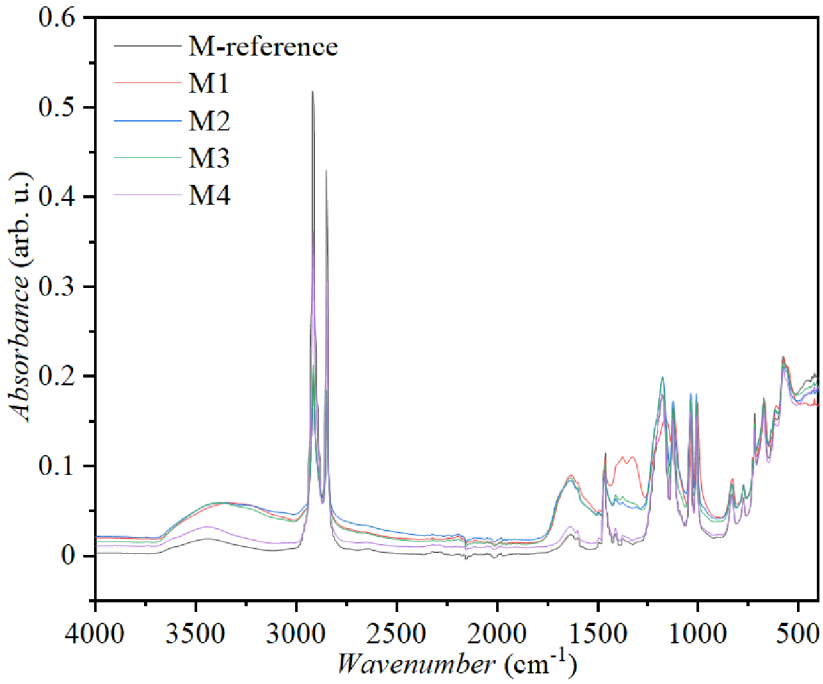

Figure 25: FTIR measurement of polymer membranes with immobilized Ag NPs and Se NPs (low-pressure plasma treatment).

Sample M - reference: pure membrane without applied NPs and without amine groups.

Sample M1: For this sample only 25 mM silver nitrate solution was used. Silver nitrate dissolves in water into Ag^{+} and NO^{3-} ions. These ions further react with the amine groups. According to the FTIR analysis, it can be seen that at the wavenumber of ≈ 3 500 cm^{-1} and in the range from ≈ 2 000 cm^{-1} to ≈ 1 000 cm^{-1} peaks with an increased intensity appeared. Thus, it can be concluded that the silver ions attached to the amine groups on the membrane formed an amide bond. In this case, the region at the ≈ 3 500 cm^{-1} represent N-H stretching and the other region from ≈ 2 000 cm^{-1} to ≈ 1 000 cm^{-1} can be assigned to secondary, primary amides and tertiary. However, in this region, peaks are not visibly sharp, most probably due to humidity of the membrane. Thus, silver ions were able to create these four types of the bindings to the membrane. Akhavan et al. reported that amine groups with silver are able to create stable silver-ammine complexes [69].

Sample M2: In this sample, silver nitrate was used as a precursor and hydrazine hydrate was used as a reductant (without stabilizing agent). From the FTIR analysis, it can be seen that immobilization of Ag NPs there was a change in the region of 3 500 cm^{-1}, similarly to sample

M1. The increased intensity also occurred at the region from ≈ 2 000 cm^{-1} to ≈ 1 000 cm^{-1}, but not as significant as in the previous sample M1. Thus, N-H stretching, primary, secondary and tertiary amide groups were formed. However, the humidity of the polymer membranes is present at the shorter wavenumber regions as in the previous sample M1.

Sample M3: Sample M3 is almost identical to sample M2. In this case, the Ag NPs were stabilized with sodium citrate. Thus, in conclusion, it seems that the stabilizing agent did not have any impact on immobilization of Ag NPs on the polymer membrane and all four types of above-mentioned amide bindings were formed (N-H stretching, primary, secondary and tertiary amides).

Sample M4: This sample corresponds to Se NPs sample A1 stabilized with PVP-29 and immobilized on polymer membrane. In this case, the intensity of the FTIR signal increased very slightly and only in the region of 3 500 cm^{-1}. Therefore, it can be assumed that the Se NPs formed only a basic amide bond (N-H stretching). As only basic amide bond was formed in this case, it can be assumed that smaller amount of Ag NPs created a bind to the polymer membrane in comparison to previous samples M1, M2 and M3, where also other types of amide bindings were formed such as primary, secondary and tertiary amides.

5.3.2 Reactive ion etching immobilization of nanoparticles on polymer membranes

In this group of samples, the amine groups were deposited by RIE with subsequent exposition to flow of ammonia gas. The particles were immobilized as in the previous case, by a wet chemical reaction, where the membranes with deposited groups were immersed directly into the reaction solution with NPs precursors, reducing and/or stabilizing agents. Subsequently, FTIR analysis was performed and the results are shown in

Figure 26.

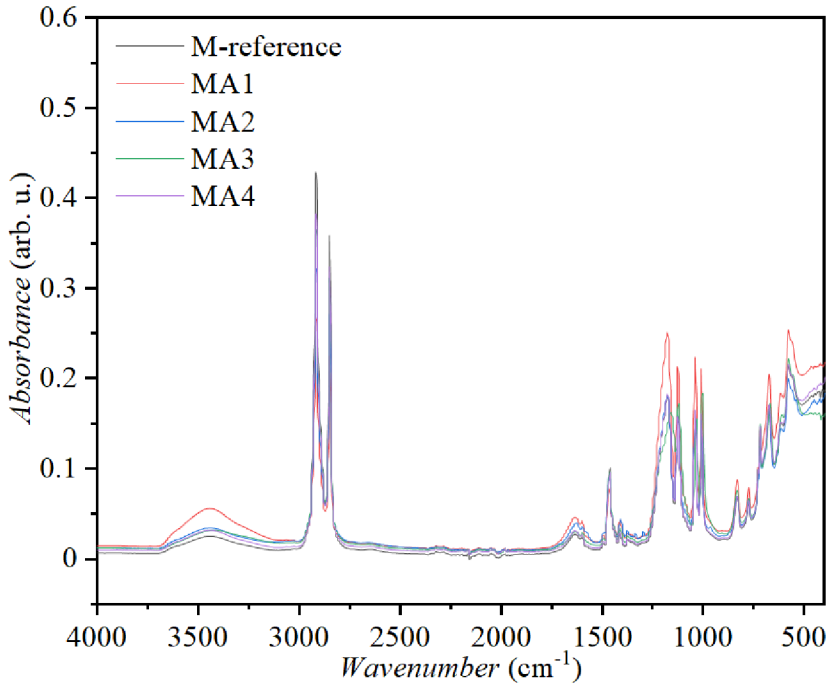

Figure 26: FTIR measurement of polymer membranes with immobilized Ag NPs and Se NPs (RIE treatment with ammonia plasma).

As can be seen from the individual spectra, all of the samples formed mainly basic amide group (N-H stretching). Since the signal intensity is quite low, it can be assumed that the binding of NPs was not that significant as in previous deposition method. However, sample MA1 shows the highest intensity, especially in the region of 3 500 cm^{-1}.

In conclusion, these the two deposition methods, namely low-pressure plasma treatment and RIE showed that immobilized NPs after low-plasma treatment were able to create variety of amide groups (basic, primary, secondary and tertiary). On the other hand, when NPs were immobilized after RIE treatment, only basic amide groups were primarily formed. It should be noted that if humidity is too high (in this case due to the wet chemical immobilization), the peaks corresponding to water molecules can overlap the areas of interest in FTIR spectra, where the amide groups are situated. FTIR spectra of both plasma deposition methods clearly show the attached humidity at the region of N-H stretching at ≈ 3 500 cm^{-1}, where the peaks are not sharp, as well as in the region of ≈ 2 000 cm^{-1} to ≈ 1 000 cm^{-1}. Additionally, membranes are fabricated from a variety of compounds such as LDPE and a filler - strong acidic or alkalic ionex based on styrene-divinylbenzene copolymer and also PES reinforcing textile. Thus, the signals from the membrane compounds can also overlap the areas in the field of interest (in this case, mostly in the region of ≈ 2 000 cm^{-1} to ≈ 1 000 cm^{-1}). In addition, immobilization of NPs on polymer membrane was performed as a wet chemical process and NPs also consist of various compounds (Ag NPs: silver nitrate, hydrazine hydrate, sodium citrate and Se NPs: sodium selenite, L-cysteine, PVP). When NPs are forming a lot of sub products can be created during the synthesis, which could also react with the deposited amine groups on the membrane and therefore have an impact on final chemical bindings between NPs and polymer membranes. Despite all of these facts, FTIR spectra clearly show the difference between individual samples, where the intensity of peaks significantly changed with immobilization of NPs on polymer membranes in comparison to a reference membrane without functional amine groups and also without NPs (sample M).

5.4 Antimicrobial activity of polymer membranes with immobilized nanoparticles

Final testing of polymer membranes with immobilized NPs was provided via macro dilution method. During this experiment samples M1 and MA4 caused high turbidity of the sample. Thus, the measurement of absorbance could be negatively affected. These samples have also changed their color from light beige to orange. It can be assumed, that the NPs immobilized on these membranes (M1 – silver nitrate, MA4 – Se NPs stabilized with PVP-29) were probably oxidized by some of the components in the liquid medium, which negatively affected the stability of the membrane and caused its degradation (dissolution). However, this problem did not occur with remaining samples (M2, M3, M4, MA1, MA2, MA3), so the measurement of absorbance was not negatively affected.

The inhibition of bacterial growth was calculated from the data of the measured turbidity (see Figure 27). The results were plotted into the bar graph in Figure 27 for a better comparison of the two bacterial cultures. All samples (except the mentioned samples with high turbidity M1 and MA4) inhibited the growth of both bacterial cultures by about 80 % except of two samples M4 (immobilized L-cysteine-reduced Se NPs stabilized with PVP-29) and MA3 (immobilized hydrazine hydrate-reduced Ag NPs stabilized with sodium citrate), which inhibited the growth of only 20-30 %. Thus, it can be said that these samples show a significant antimicrobial effect.

Sample M4 represents Se NPs (A1-stabilized with PVP-29) deposited with low-pressure plasma treatment of polymer membrane. In sample MA3 are Ag NPs stabilized with sodium citrate and the polymer membrane was treated with RIE and ammonia plasma. In this case, there are few possible reasons, why the antimicrobial effect was lower than for the other samples. It could by caused by lower amount of immobilized NPs on the polymer membrane or due to the bonding, which changed the antimicrobial properties of these samples.

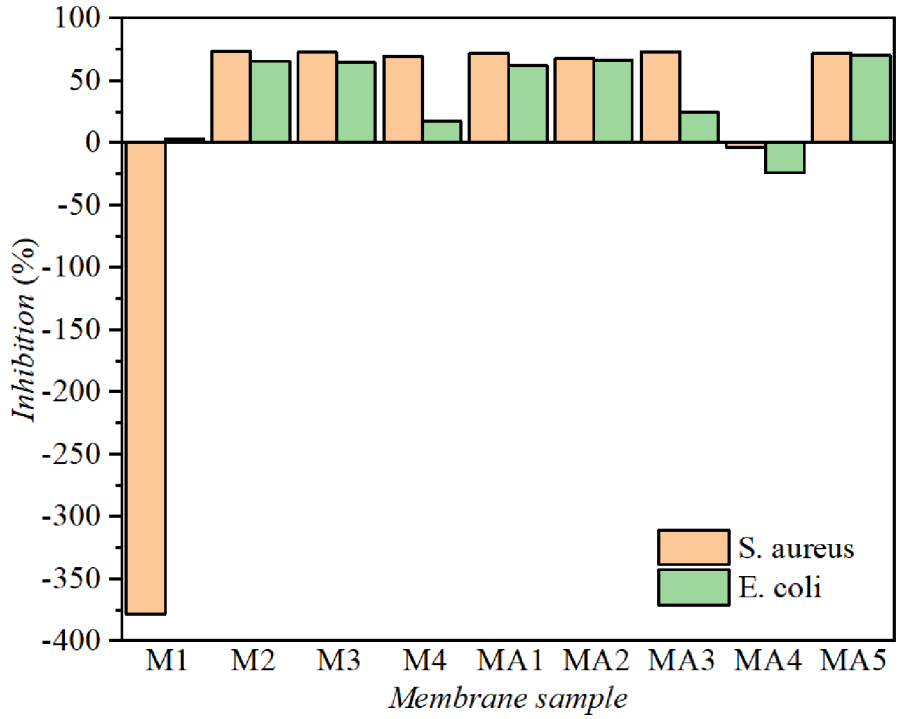

Figure 27: Inhibition after 24 h - immobilized NPs on polymer membranes applied against S. aureus and E. coli

In summary, these experiments showed that the bindings formed between the NPs and the polymer membrane have a significant importance for the final antimicrobial effect. It could be assumed that there could be a synergistic effect of the polymer membrane with bonded NPs and this antimicrobial effect was enhanced in comparison to antimicrobial tests performed on pure NPs (where mostly bacteriostatic effect occurred). It could also be assumed that the type of bond (basic, primary, secondary or tertiary amide) does not affect the antimicrobial efficacy. As well as the deposition method to functionalize the polymers does not have any significant effect on final antimicrobial properties of polymer membranes with immobilized NPs.

In conclusion, it would be appropriate to consider the antimicrobial action of the polymer membrane with immobilized NPs. From the above-mentioned antimicrobial tests, which were performed only on NPs, it was clear that NPs showed more bacteriostatic rather than a bactericidal effect. However, when individual parts of the polymer membranes with immobilized NPs are taken into account, it is not just the NPs that can affect the bacteria. It is necessary to consider also the plasma modification of the membrane, where new functional groups and other highly reactive species have been formed and also the binding between NPs and the membrane, as well as the NPs themselves. Thus, each of these aspects may affect the final antimicrobial properties of as prepared samples.

The synergistic effect of polymer and NPs could also be considered. Here, two interesting scientific papers should be noted. The first, published by Pekárková et al., where Se NPs were used to modify parylene-C micropillars for antimicrobial effect resulting in very low efficacy against *S. aureus* and *E. coli*. They found out that micropillars could have a negative effect against cell cultures [86]. The second scientific paper published by our team (Gablech E. et al.), where a synergistic effect of Se NPs stabilized with PVP-29 mixed with commercial antifungal product was investigated [87]. When Se NPs were mixed with commercial antifungal product, it can be assumed that new chemical bindings between these two compounds were formed. The results showed that this mixture was more effective against fungus *Serpula lacrymans* rather than used individually. Thus, it can be considered that chemical binding between NPs and polymer membrane can potentially affect the final antimicrobial effect.

6 Conclusion

The main objective of the dissertation thesis was to improve antimicrobial efficiency of commercial polymer membranes used in the food industry for the filtration of milk products, especially whey. These membranes suffer from microbial contamination, which negatively affects not only the filtration process itself but also significantly reduces the life-time of this membrane. Therefore, the aim of this work was to immobilize the suitable antimicrobial NPs on the polymer membrane to achieve antimicrobial properties and thus to protect the membrane from formation of biofilm of microorganisms present in milk and whey. Among various types of NPs exhibiting strong antimicrobial properties, Ag NPs and Se NPs seem to be the most effective antimicrobial agents as reported in the literature. Thus, these NPs were utilized for immobilization on the polymer membrane treated with plasma for deposition of functional amine groups. These groups enabled binding of NPs to membrane by forming amide groups. Such functionalized membranes were tested for antimicrobial properties.

Specific objective 1: Synthesis of NPs

This part of work was devoted to optimization of the preparation processes of individual types of NPs, specifically Ag NPs and Se NPs. Various procedures and factors that could affect the final biological and physico-chemical properties of NPs have been investigated. These factors include various precursors, reducing and stabilizing agents, or physical factors such as temperature or UV-irradiation. Furthermore, the effect of their concentration and also their various combinations were investigated.

Silver nanoparticles

The most suitable synthesis of Ag NPs was when Ag NPs were reduced by hydrazine hydrate employing UV-irradiation with different wavelengths, namely 255 nm, 366 nm and 400 nm. A control sample without any radiation was also prepared in the dark environment. It was found that UV radiation was also very important factor that can affect final properties of Ag NPs, especially the shape and size. With increasing wavelengths of UV radiation, the shape of Ag NPs changed from spherical to anisotropic (various shapes as rods, triangular plates with truncated tops, spheres). The stability of the particles was also significantly prolonged (including the control sample prepared in darkness) up to 3 weeks after synthesis, which was also confirmed by UV-VIS spectroscopy analysis.

Selenium nanoparticles

Similarly, to Ag NPs, the synthesis of Se NPs was optimized and several factors were investigated. This method was invented and optimized in our laboratory. Sodium selenite was used as precursor, L-cysteine was reducing agent and three different stabilizers were used in this synthesis: PVP-29, PVP-40 and BSA. The shape of all types of Se NPs samples was spherical and the stability of these particles was also sufficient (no sediments were seen 2 weeks after synthesis). Subsequent analyzes showed that the various stabilizing agents affected mainly the size of Se NPs. Se NPs stabilized with PVP-29 evinced the smallest size around 40 nm confirmed by STEM and SAXS. Because of the smallest dimensions, Se NPs stabilized with PVP-29 (sample A1) was selected for further experiments, i.e. for immobilization on membrane to achieve its antimicrobial coating.

Specific objective 2: Cytotoxicity of NPs

Silver nanoparticles

Following samples of Ag NPs were tested with MTT assay to determine their cytotoxicity: sample A prepared under UV light of 255 nm, sample B prepared under UV light of 366 nm and sample C prepared under UV light of 400 nm, and sample X prepared in darkness. However, in this part of the work, an obstacle with the stability of Ag NPs occurred. When Ag NPs were dispersed in DMEM medium (originally dispersed in deionized water), Ag NPs rapidly agglomerated (big agglomerates could be seen by naked eye). This problem was partially solved with utilization of ultrasonic bath, which helped to improve their stability for 24 h. After this period big agglomerates appeared again at the bottom of the vessel. Another problem was the preparation of Ag NPs for this assay - Ag NPs were centrifuged and then dried in a small Petri dish to determine the specific concentration and subsequent dilution. However, the yield of Ag NPs was very small and it was difficult to separate Ag NPs from the Petri dish. However, this analysis showed, although only partially, that with increasing concentration (from 2.5 mg/ml to 220 mg/ml), their toxicity, e.g. cell viability decreased.

Selenium nanoparticles

Two assays were performed to determine the cytotoxicity of Se NPs, namely the XTT cytotoxicity assay and the BrdU proliferation assay. The results of these assays showed interesting results. At higher concentrations, Se NPs (2 mg/ml and 5 mg ml) showed a significant cytotoxic effect. However, with decreasing concentration, they promoted cell growth. This could be explained by the fact that Se is a micronutrient, and at very low concentrations may support some of the cellular processes.

Specific objective 3: Antimicrobial activity of NPs

Silver nanoparticles

Measurement of growth curves showed only partial inhibition of the growth of both bacterial cultures. The third, dilution method confirmed the antimicrobial properties for both bacterial clusters, but more significantly against *S. aureus* culture, where Ag NPs samples A (prepared under UV light of 255 nm) and C (prepared under UV light of 400 nm) inhibited the growth of bacteria by about 50 %, while for *E. coli* only about 30 %. However, from all the performed tests, it was obvious that none of the samples with any concentration was able to completely inhibit the growth of bacterial cultures, which would indicate rather a bacteriostatic than a bactericidal effect.

Selenium nanoparticles

Antimicrobial activity Se NPs were tested on three samples, A1 (stabilized with PVP-29), A2 (stabilized with PVP-40) and A3 (stabilized with BSA). The MIC and growth curves measurements were used to observe the antimicrobial effect. Measurements were performed on two bacterial cultures, *E. coli* and *S. aureus*. The results showed that, similarly to Ag NPs, none of the samples was able to completely inhibit the growth of both bacterial cultures. Again, it can be assumed that Se NPs exhibit antimicrobial properties with a bacteriostatic effect. An interesting phenomenon was also found with testing of *S. aureus* bacterial culture: with increasing concentration of Se NPs, the antimicrobial effect decreased. These results were confirmed by both types of antimicrobial methods.

Specific objective 4: Plasma treatment of polymer membranes and immobilization of NPs

This part of the work was focused on plasma modification of polymer membranes and deposition of amine functional groups and subsequent immobilization of Ag NPs and Se NPs. Two different approaches were used: low-pressure plasma deposition with CPA polymerization and RIE with ammonia plasma utilization. Due to the low stability of the functional groups, the NPs were immobilized immediately after plasma treatment by a wet chemical reaction, i.e. by immersing the membrane directly in the reaction solution of the NPs. It was found that UV-radiation, used for Ag NPs synthesis, had a negative effect on the stability of the membrane, which began to dissolve. Therefore, a new series of experiments was performed. Due to antimicrobial tests of Ag NPs, which showed that the composition of Ag NPs, e.g. silver nitrate, hydrazine hydrate and sodium citrate exhibited antimicrobial properties, the effect of these individual components, which were immobilized on the membrane, was investigated. The Se NPs of sample A1 (stabilized with PVP-29) were also immobilized on a membrane.

The results of FTIR analysis showed that all types of binded NPs formed different types of amide binds - basic, primary, secondary and tertiary. Low-pressure plasma treatment proved to be a more suitable way of membrane modification than RIE with ammonia plasma because in case of utilization of low-pressure plasma, NPs were able to form different types of amide bonds from basic to tertiary, while in case of utilization of RIE with ammonia plasma only basic amide binds.

Specific objective 5: Antimicrobial activity of polymer membranes with immobilized NPs

The antimicrobial activity of the polymer membrane with immobilized NPs was tested by a microdilution method against bacterial strains *S. aureus* and *E. coli*. The results showed that NPs immobilized by both types of plasma modification of polymer membrane evinced a strong inhibitory effect on both bacterial cultures. It was also found that all membranes with immobilized NPs (except for samples M1 and MA4 since the immersion of the membranes into medium caused their dissolution and abnormal turbidity of samples) evinced strong antimicrobial effect against both bacterial cultures and inhibited their growth by about 80 %. However, it was found out that the immobilized NPs on the polymer membrane showed significantly higher antimicrobial effect than the NPs applied themselves (confirmed by antimicrobial tests).

In conclusion, this dissertation thesis required interdisciplinary approach as several different areas were investigated such as NPs synthesis and optimization, polymer treatment by plasma, testing of cytotoxicity and antimicrobial properties. Several challenging issues occurred during the experiments - especially linked with the stability of the membrane and the stability of the NPs themselves. The annex polymer membrane dissolved in some reagents, and therefore only a catex membrane was used for all types of experiments because it showed slightly better stability. The membrane also caused problems when analyzed with vacuum methods - it extensively released a gas and therefore, it was necessary to pump the chamber for a very long time to achieve a suitable level of vacuum. Finally, when NPs were immobilized on the surface of the membrane by the wet chemical process, the membrane swelled and a significant moisture remained absorbed in the membrane, which made it difficult to interpret the FTIR results, Therefore, the membrane samples with immobilized NPs had to be kept in a dry box for a month. A large number of experiments and subsequent analyzes have been performed, which have shown that both Se NPs and Ag NPs can evince strong antimicrobial effect. It was also found that antimicrobial activity can be significantly affected by the binding of NPs to membrane and also synergistic effect could be considered. According to antimicrobial tests of polymer membranes with immobilized NPs, the antimicrobial effect is affected not only by NPs per se but also by plasma treated membrane, its functional groups and other highly reactive species that were formed during this treatment.

7 References

1. Daufin, G., et al., *Recent and emerging applications of membrane processes in the food and dairy industry.* Food and Bioproducts Processing, 2001. **79**(2): p. 89-102.
2. Pouliot, Y., *Membrane processes in dairy technology—From a simple idea to worldwide panacea.* International Dairy Journal, 2008. **18**(7): p. 735-740.
3. Aguero, R., et al., *Membrane processes for whey proteins separation and purification. A review.* Current Organic Chemistry, 2017. **21**(17): p. 1740-1752.
4. Wen-Qiong, W., et al., *Whey protein membrane processing methods and membrane fouling mechanism analysis.* Food chemistry, 2019. **289**: p. 468-481.
5. Kowalik-Klimczak, A., *The possibilities of using membrane filtration in the dairy industry.* Journal of Machine Construction and Maintenance-Problemy Eksploatacji, 2017.
6. Kumar, P., et al., *Perspective of membrane technology in dairy industry: A review.* Asian-Australasian Journal of Animal Sciences, 2013. **26**(9): p. 1347.
7. Charcosset, C., *Classical and recent applications of membrane processes in the food industry.* Food Engineering Reviews, 2021. **13**(2): p. 322-343.
8. Chamberland, J., et al., *Biofouling of ultrafiltration membrane by dairy fluids: Characterization of pioneer colonizer bacteria using a DNA metabarcoding approach.* Journal of dairy science, 2017. **100**(2): p. 981-990.
9. Kaur, N., et al., *Recent developments in purification techniques and industrial applications for whey valorization: A review.* Chemical Engineering Communications, 2020. **207**(1): p. 123-138.
10. Anand, S. and D. Singh, *Resistance of the constitutive microflora of biofilms formed on whey reverse-osmosis membranes to individual cleaning steps of a typical clean-in-place protocol.* Journal of dairy science, 2013. **96**(10): p. 6213-6222.
11. Sun, X.-F., et al., *Graphene oxide–silver nanoparticle membrane for biofouling control and water purification.* Chemical Engineering Journal, 2015. **281**: p. 53-59.
12. Saion, E., E. Gharibshahi, and K. Naghavi, *Size-controlled and optical properties of monodispersed silver nanoparticles synthesized by the radiolytic reduction method.* International journal of molecular sciences, 2013. **14**(4): p. 7880-7896.
13. Zain, N.M., A.G.F. Stapley, and G. Shama, *Green synthesis of silver and copper nanoparticles using ascorbic acid and chitosan for antimicrobial applications.* Carbohydrate Polymers, 2014. **112**(0): p. 195-202.
14. Abou El-Nour, K.M.M., et al., *Synthesis and applications of silver nanoparticles.* Arabian Journal of Chemistry, 2010. **3**(3): p. 135-140.
15. Prabhu, S. and E. Poulose, *Silver nanoparticles: mechanism of antimicrobial action, synthesis, medical applications, and toxicity effects.* International Nano Letters, 2012. **2**(1): p. 1-10.
16. Tran, Q.H. and A.-T. Le, *Silver nanoparticles: synthesis, properties, toxicology, applications and perspectives.* Advances in Natural Sciences: Nanoscience and Nanotechnology, 2013. **4**(3): p. 033001.
17. Shameli, K., et al., *Investigation of antibacterial properties silver nanoparticles prepared via green method.* Chemistry Central Journal, 2012. **6**(1): p. 73.
18. Nayak, V., et al., *Potentialities of selenium nanoparticles in biomedical science.* New Journal of Chemistry, 2021. **45**(6): p. 2849-2878.
19. Guzmán, M.G., J. Dille, and S. Godet, *Synthesis of silver nanoparticles by chemical reduction method and their antibacterial activity.* Int J Chem Biomol Eng, 2009. **2**(3): p. 104-111.
20. Kalaivani, R., et al., *Synthesis of chitosan mediated silver nanoparticles (Ag NPs) for potential antimicrobial applications.* Frontiers in Laboratory Medicine, 2018. **2**(1): p. 30-35.
21. Luo, S., et al., *In situ and controllable synthesis of Ag NPs in tannic acid-based hyperbranched waterborne polyurethanes to prepare antibacterial polyurethanes/Ag NPs composites.* RSC advances, 2018. **8**(64): p. 36571-36578.
22. Ottoni, C., et al., *Environmental impact of biogenic silver nanoparticles in soil and aquatic organisms.* Chemosphere, 2020. **239**: p. 124698.

23. Tran, P.A. and T.J. Webster, *Selenium nanoparticles inhibit Staphylococcus aureus growth.* International journal of nanomedicine, 2011. **6**: p. 1553.
24. Medina Cruz, D., G. Mi, and T.J. Webster, *Synthesis and characterization of biogenic selenium nanoparticles with antimicrobial properties made by Staphylococcus aureus, methicillin-resistant Staphylococcus aureus (MRSA), Escherichia coli, and Pseudomonas aeruginosa.* Journal of Biomedical Materials Research Part A, 2018. **106**(5): p. 1400-1412.
25. MemBrain, s.r.o. 2021 [cited 2021; Available from: https://www.membrain.cz/.
26. Jiránková, H., *Membránové procesy v potravinářství a mlékárenství.* Pardubice: Ústav environmentálního a chemického inženýrství, UPa,[cit. 2017-06-06]. Dostupný z http://www. czemp. cz/sites/default/files/clanek/1071/prilohy/1. mempro-mlk. pdf.
27. Selatile, M.K., et al., *Recent developments in polymeric electrospun nanofibrous membranes for seawater desalination.* RSC advances, 2018. **8**(66): p. 37915-37938.
28. Honarparvar, S., et al., *Frontiers of Membrane Desalination Processes for Brackish Water Treatment: A Review.* Membranes, 2021. **11**(4): p. 246.
29. Bernauer, B., et al., *Membránové procesy.* 1 ed. 2012, Praha: VŠCHT. 296.
30. Ečer, J.a.K., J. *Membránové procesy v mlékárenském průmyslu.* Mlékárenské listy, 2014. **č. 145**.
31. Křivčík, J., *Iontově selektivní membrány.* 2013, MemBrain, s.r.o. p. 44.
32. Bansal, B. and X.D. Chen, *A critical review of milk fouling in heat exchangers.* Comprehensive reviews in food science and food safety, 2006. **5**(2): p. 27-33.
33. Akar, N., et al., *Investigation of characterization and biofouling properties of PES membrane containing selenium and copper nanoparticles.* Journal of Membrane Science, 2013. **437**: p. 216-226.
34. Kochkodan, V. and N. Hilal, *A comprehensive review on surface modified polymer membranes for biofouling mitigation.* Desalination, 2015. **356**: p. 187-207.
35. Sedlarik, V., *Antimicrobial modifications of polymers.* Biodegradation-Life of Science, 2013: p. 187-204.
36. Zhu, J., et al., *Polymeric antimicrobial membranes enabled by nanomaterials for water treatment.* Journal of Membrane Science, 2018. **550**: p. 173-197.
37. Mijnendonckx, K., et al., *Antimicrobial silver: uses, toxicity and potential for resistance.* Biometals, 2013. **26**(4): p. 609-621.
38. Zhang, X.-F., et al., *Silver nanoparticles: synthesis, characterization, properties, applications, and therapeutic approaches.* International journal of molecular sciences, 2016. **17**(9): p. 1534.
39. Durán, N., et al., *Silver nanoparticles: A new view on mechanistic aspects on antimicrobial activity.* Nanomedicine: nanotechnology, biology and medicine, 2016. **12**(3): p. 789-799.
40. Cha, S.-H., et al., *Shape-dependent biomimetic inhibition of enzyme by nanoparticles and their antibacterial activity.* ACS nano, 2015. **9**(9): p. 9097-9105.
41. Mohan, S., et al., *Completely green synthesis of dextrose reduced silver nanoparticles, its antimicrobial and sensing properties.* Carbohydrate Polymers, 2014. **106**(0): p. 469-474.
42. Yin, J., et al., *Attachment of silver nanoparticles (AgNPs) onto thin-film composite (TFC) membranes through covalent bonding to reduce membrane biofouling.* Journal of membrane science, 2013. **441**: p. 73-82.
43. Haider, M.S., et al., *Aminated polyethersulfone-silver nanoparticles (AgNPs-APES) composite membranes with controlled silver ion release for antibacterial and water treatment applications.* Materials Science and Engineering: C, 2016. **62**: p. 732-745.
44. Das, R., S. Gang, and S.S. Nath, *Preparation and antibacterial activity of silver nanoparticles.* Journal of Biomaterials and nanobiotechnology, 2011. **2**: p. 472.
45. Geoffrion, L.D., et al., *Naked selenium nanoparticles for antibacterial and anticancer treatments.* ACS omega, 2020. **5**(6): p. 2660-2669.
46. Guisbiers, G., et al., *Inhibition of E. coli and S. aureus with selenium nanoparticles synthesized by pulsed laser ablation in deionized water.* International journal of nanomedicine, 2016. **11**: p. 3731.
47. Xu, C., et al., *Biogenic synthesis of novel functionalized selenium nanoparticles by Lactobacillus casei ATCC 393 and its protective effects on intestinal barrier dysfunction caused by enterotoxigenic Escherichia coli K88.* Frontiers in microbiology, 2018. **9**: p. 1129.

48. Ahmed, M., et al., *Wound dressing properties of functionalized environmentally biopolymer loaded with selenium nanoparticles.* Journal of Molecular Structure, 2021. **1225**: p. 129138.
49. Khiralla, G.M. and B.A. El-Deeb, *Antimicrobial and antibiofilm effects of selenium nanoparticles on some foodborne pathogens.* LWT-Food Science and Technology, 2015. **63**(2): p. 1001-1007.
50. Filipović, N., et al., *Comparative study of the antimicrobial activity of selenium nanoparticles with different surface chemistry and structure.* Frontiers in bioengineering and biotechnology, 2021. **8**: p. 1591.
51. Huang, T., et al., *Engineering highly effective antimicrobial selenium nanoparticles through control of particle size.* Nanoscale, 2019. **11**(31): p. 14937-14951.
52. Escobar-Ramírez, M.C., et al., *Antimicrobial activity of Se-nanoparticles from bacterial biotransformation.* Fermentation, 2021. **7**(3): p. 130.
53. Kailasa, S.K., et al., *Antimicrobial activity of silver nanoparticles*, in *Nanoparticles in pharmacotherapy*. 2019, Elsevier. p. 461-484.
54. Palza, H., *Antimicrobial polymers with metal nanoparticles.* International journal of molecular sciences, 2015. **16**(1): p. 2099-2116.
55. Mikhailova, E.O., *Silver Nanoparticles: Mechanism of action and probable bio-application.* Journal of Functional Biomaterials, 2020. **11**(4): p. 84.
56. Yin, I.X., et al., *The antibacterial mechanism of silver nanoparticles and its application in dentistry.* International journal of nanomedicine, 2020. **15**: p. 2555.
57. Ahmad, S.A., et al., *Bactericidal activity of silver nanoparticles: a mechanistic review.* Materials Science for Energy Technologies, 2020.
58. Steve, W. and W. Thomas, *Efficacy and mechanism of selenium nanoparticles as antibacterial agents.* Frontiers in Bioengineering and Biotechnology, 2016. **4**.
59. Truong, L.B., et al., *Selenium Nanomaterials to Combat Antimicrobial Resistance.* Molecules, 2021. **26**(12): p. 3611.
60. Chan, C.-M., T.-M. Ko, and H. Hiraoka, *Polymer surface modification by plasmas and photons.* Surface science reports, 1996. **24**(1-2): p. 1-54.
61. Qi, L., et al., *Polymeric membrane ion-selective electrodes with anti-biofouling properties by surface modification of silver nanoparticles.* Sensors and Actuators B: Chemical, 2021. **328**: p. 129014.
62. Manakhov, A., et al., *Carboxyl-anhydride and amine plasma coating of PCL nanofibers to improve their bioactivity.* Materials & Design, 2017. **132**: p. 257-265.
63. Manakhov, A., et al., *Deposition of stable amine coating onto polycaprolactone nanofibers by low pressure cyclopropylamine plasma polymerization.* Thin Solid Films, 2015. **581**: p. 7-13.
64. Oehr, C., *Plasma surface modification of polymers for biomedical use.* Nuclear Instruments and Methods in Physics Research Section B: Beam Interactions with Materials and Atoms, 2003. **208**: p. 40-47.
65. Liston, E., L. Martinu, and M. Wertheimer, *Plasma surface modification of polymers for improved adhesion: a critical review.* Journal of adhesion science and technology, 1993. **7**(10): p. 1091-1127.
66. Kochkodan, V.M. and V.K. Sharma, *Graft polymerization and plasma treatment of polymer membranes for fouling reduction: A review.* Journal of Environmental Science and Health, Part A, 2012. **47**(12): p. 1713-1727.
67. Tylkowski, B., et al., *Applications of silver nanoparticles stabilized and/or immobilized by polymer matrixes.* Physical Sciences Reviews, 2017. **2**(7).
68. Park, S.-H., et al., *Direct incorporation of silver nanoparticles onto thin-film composite membranes via arc plasma deposition for enhanced antibacterial and permeation performance.* Journal of membrane science, 2016. **513**: p. 226-235.
69. Akhavan, B., et al., *Direct covalent attachment of silver nanoparticles on radical-rich plasma polymer films for antibacterial applications.* Journal of Materials Chemistry B, 2018. **6**(37): p. 5845-5853.
70. Brewis, D., *Adhesion to polymers: how important are weak boundary layers?* International journal of adhesion and adhesives, 1993. **13**(4): p. 251-256.
71. Yasuda, H., *Plasma for modification of polymers.* Journal of Macromolecular Science—Chemistry, 1976. **10**(3): p. 383-420.

72. Jiang, H., et al., *Plasma-enhanced deposition of silver nanoparticles onto polymer and metal surfaces for the generation of antimicrobial characteristics.* Journal of Applied Polymer Science, 2004. **93**(3): p. 1411-1422.
73. Airoudj, A., L. Ploux, and V. Roucoules, *Effect of plasma duty cycle on silver nanoparticles loading of cotton fabrics for durable antibacterial properties.* Journal of Applied Polymer Science, 2015. **132**(1).
74. Hosseini, S., et al., *Preparation and surface modification of PVC/SBR heterogeneous cation exchange membrane with silver nanoparticles by plasma treatment.* Journal of Membrane Science, 2010. **365**(1-2): p. 438-446.
75. Taheri, S., et al., *Binding of nanoparticles to aminated plasma polymer surfaces is controlled by primary amine density and solution PH.* The Journal of Physical Chemistry C, 2018. **122**(26): p. 14986-14995.
76. Agnihotri, S., S. Mukherji, and S. Mukherji, *Immobilized silver nanoparticles enhance contact killing and show highest efficacy: elucidation of the mechanism of bactericidal action of silver.* Nanoscale, 2013. **5**(16): p. 7328-7340.
77. McMichael, K. *Amines- Reactions* 2021 [cited 2022; Available from: https://chem.libretexts.org/Bookshelves/Organic_Chemistry/Book%3A_Organic_Chemistry_-_A_Carbonyl_Early_Approach_(McMichael)/01%3A_Chapters/1.20%3A_Amines-_Reactions.
78. Darroudi, M., et al., *Fabrication and characterization of gelatin stabilized silver nanoparticles under UV-light.* International journal of molecular sciences, 2011. **12**(9): p. 6346-6356.
79. Stamplecoskie, K.G. and J.C. Scaiano, *Light emitting diode irradiation can control the morphology and optical properties of silver nanoparticles.* Journal of the American Chemical Society, 2010. **132**(6): p. 1825-1827.
80. Graves Jr, J.L., et al., *Rapid evolution of silver nanoparticle resistance in Escherichia coli.* Frontiers in genetics, 2015. **6**: p. 42.
81. Srivastava, G.K., et al., *Comparison between direct contact and extract exposure methods for PFO cytotoxicity evaluation.* Scientific Reports, 2018. **8**(1): p. 1-9.
82. Crane, A.M. and S.K. Bhattacharya, *The use of bromodeoxyuridine incorporation assays to assess corneal stem cell proliferation*, in *Corneal Regenerative Medicine*. 2013, Springer. p. 65-70.
83. Shahid, M., et al., *A critical review of selenium biogeochemical behavior in soil-plant system with an inference to human health.* Environmental Pollution, 2018. **234**: p. 915-934.
84. Ramos, J.F. and T.J. Webster, *Cytotoxicity of selenium nanoparticles in rat dermal fibroblasts.* International journal of nanomedicine, 2012. **7**: p. 3907.
85. León-Mancilla, B., et al., *Physico-chemical characterization of collagen scaffolds for tissue engineering.* Journal of applied research and technology, 2016. **14**(1): p. 77-85.
86. Pekarkova, J., et al., *Modifications of Parylene by Microstructures and Selenium Nanoparticles: Evaluation of Bacterial and Mesenchymal Stem Cell Viability.* Frontiers in Bioengineering and Biotechnology, 2021. **9**.
87. Gablech, E., et al., *Selenium nanoparticles with boron salt-based compound act synergistically against the brown-rot Serpula lacrymans.* International Biodeterioration & Biodegradation, 2022. **169**: p. 105377.